HYPER VERSION

Received: *October 17, 2000*, Accepted: *November 01, 2000*

Transport coefficients in high temperature gauge theories, 1. Leading-log results

Peter Arnold

Department of Physics, University of Virginia
Charlottesville, VA 22901, USA
E-mail: parnold@virginia.edu

Guy David Moore and Laurence G. Yaffe

Department of Physics, University of Washington
Seattle, Washington 98195, USA
E-mail: guymoore@phys.washington.edu,
yaffe@phys.washington.edu

Abstract: Leading-log results are derived for the shear viscosity, electrical conductivity and flavor diffusion constants in both abelian and non-abelian high temperature gauge theories with various matter field content.

Keywords: Baryogenesis, Thermal Field Theory, Physics of the Early Universe.

JHEP11(2000)001

Contents

JHEP11(2000)001

1. Introduction and summary

Transport coefficients, such as viscosities, diffusivities or conductivity, characterize the dynamics of long wavelength, low frequency fluctuations in a medium. In condensed matter applications transport coefficients are typically measured, not calculated from first principles, due to the complexity of the underlying microscopic dynamics. But in a weakly coupled quantum field theory, transport coefficients should, in principle, be calculable purely theoretically. Knowledge of various transport coefficients in high temperature gauge theories is important in cosmological applications such as electroweak baryogenesis [1, 2], as well as hydrodynamic models of heavy ion collisions [3].

In this paper, we consider the evaluation of transport coefficients in weakly coupled high temperature gauge theories. "High temperature" is taken to mean that the temperature is much larger than the zero-temperature masses of elementary particles and any chemical potentials. In QED, this means $T \gg m_e$, while in QCD, we require both $T \gg \Lambda_{\rm QCD}$ and $T \gg m_q$. Corrections suppressed by powers of temperature (m_q/T, $\Lambda_{\rm QCD}/T$, etc.) will be ignored. This means that each transport coefficient will equal some power of temperature, trivially determined by dimensional analysis, multiplied by some function of the dimensionless coupling constants of the theory.

As an example, the shear viscosity in a (single component, real) $\frac{\lambda}{4!}\phi^4$ scalar theory has the high temperature form

$$\eta = a \, \frac{T^3}{\lambda^2} \,, \tag{1.1}$$

with $a = 3033.5$, up to relative corrections suppressed by higher powers of λ [4, 5].[1] The leading $1/\lambda^2$ behavior reflects the fact that the two-body scattering cross section is $O(\lambda^2)$, and that transport coefficients are inversely proportional to scattering rates.

In gauge theories, the presence of Coulomb scattering over a parametrically wide range of momentum transfers (or scattering angles) causes transport coefficients to have a more complicated dependence on the interaction strength. In QED, for example, the high temperature shear viscosity has the form

$$\eta = \kappa \, \frac{T^3}{\alpha^2 \, \ln \alpha^{-1}} \,, \tag{1.2}$$

up to relative corrections which are suppressed by additional factors of $1/\ln\alpha^{-1}$. Evaluating the overall constant κ, while ignoring all terms suppressed by additional powers of $1/\ln\alpha^{-1}$ (or powers of α) amounts to a "leading-log" calculation of the transport coefficient.

In this paper, we will present leading-log calculations of the shear viscosity, electrical conductivity and flavor diffusion constants in high temperature gauge theories (abelian or non-abelian) with various matter field content.[2] It should be emphasized, however, that these leading-log results cannot be presumed to provide a quantitatively reliable determination of transport coefficients in any real application. Gauge couplings in the standard model are never so tiny that corrections suppressed by

[1] The value quoted for a actually comes from our own evaluation of the ϕ^4 shear viscosity, using the variational formulation described in section 2. This allows a higher precision evaluation than that obtained by discretizing the requisite integral equation as described in [5].

[2] We will not consider the bulk viscosity. It requires a significantly different and more complicated, analysis than other transport coefficients. We also do not treat thermal conductivity, which is not an independent transport coefficient in the absence of non-zero conserved charges (besides energy and momentum).

$1/\ln\alpha_{\rm s}^{-1}$, $1/\ln\alpha_{\rm w}^{-1}$ or even $1/\ln\alpha_{\rm EM}^{-1}$ are negligibly small. Nevertheless, the leading-log analysis of transport coefficients is a useful first step. In a companion paper, we extend our treatment and obtain "all-log" results which include all terms suppressed only by inverse logarithms of the gauge coupling (but drop sub-leading effects suppressed by powers of the coupling) [6].

Previous efforts to determine transport coefficients in hot gauge theories include many applications of *relaxation time* approximations [7]–[16], in which the full momentum dependence of relevant scattering rates are crudely characterized by a single relaxation time. Such treatments can, at best, obtain the correct leading parametric dependence on the coupling and a rough estimate of the overall coefficient (though some of them [13]–[16] do not obtain the right parametric behavior). In addition, there have been a number of papers reporting genuine leading-log evaluations of various transport coefficients [17]–[23]. However, we find that almost all of these results are incorrect due to a variety of both conceptual and technical errors. (In some cases [17], the errors are numerically quite small.) For each transport coefficient we consider, specific comparisons with previous work will be detailed in the relevant section below.

In section 2 we discuss how one may construct a linearized kinetic theory which is adequate for computing correctly the transport coefficients we consider, up to corrections suppressed by powers of coupling. We also show how the actual calculation of a transport coefficient may be converted into a variational problem; this is very convenient for numerical purposes. (Related, but somewhat different variational formulations appear in the literature.) For leading-log calculations one may greatly simplify the resulting collision integrals, since the coefficient of the leading-log is only sensitive to small angle scattering processes. This is discussed in section 3. The details of the analysis for the electrical conductivity, flavor diffusivities and shear viscosity are presented in sections 4, 5 and 6, respectively. Throughout this paper, we will present results for arbitrary simple gauge groups, rather than specializing to SU(N). Our notation for group factors ($C_{\rm R}$, $T_{\rm R}$, $d_{\rm R}$), their SU(N) values, and how to interpret them for abelian problems, is explained in appendix A.

In the remainder of this introduction, we review the basic definitions of the various transport coefficients and then summarize our results.

1.1 Definitions

At sufficiently high temperature, the equilibrium state of any relativistic field theory may be regarded as a relativistic fluid. The stress energy tensor $T_{\mu\nu}$ defines four locally-conserved currents whose corresponding conserved charges are, of course, the total energy and spatial momentum of the system. At any point in the system, the local fluid rest frame is defined as the frame in which the local momentum density vanishes,[3]

$$T^0_{\ i}(x) = 0 \qquad \Longleftrightarrow \qquad [\text{local fluid rest frame at } x]\,. \tag{1.3}$$

If the fluid is slightly disturbed from equilibrium, then the non-equilibrium expectation of $T_{\mu\nu}$, in the local fluid rest frame, satisfies the constitutive relation[4]

$$\langle T_{ij}\rangle = \delta_{ij}\,\langle \mathcal{P}\rangle - \eta \left[\nabla_i\, u_j + \nabla_j\, u_i - \frac{2}{3}\,\delta_{ij}\,\nabla^l\, u_l\right] - \zeta\,\delta_{ij}\,\nabla^l\, u_l\,, \tag{1.4}$$

together with the exact conservation law $\partial_\mu \langle T^{\mu\nu}\rangle = 0$. In the constitutive relation (1.4), η is the *shear viscosity*, ζ is the *bulk viscosity* and $\mathbf{u}$ is local flow velocity. For small departures from equilibrium,

$$u_i \equiv \frac{\langle T^0_{\ i}\rangle}{\langle \varepsilon + \mathcal{P}\rangle}\,, \tag{1.5}$$

where $\varepsilon \equiv T^{00}$ is the energy density and $\mathcal{P} \equiv \frac{1}{3} T^i_{\ i}$ the (local) pressure. The combination $\varepsilon + \mathcal{P}$ is also known as the enthalpy. The constitutive relation (1.4) holds up to corrections involving further gradients or higher powers of $\mathbf{u}$.

In a similar fashion, in any theory containing electromagnetism (i.e. a U(1) gauge field), the electric current density $j^{\rm EM}_\mu$ is conserved ($\partial^\mu j^{\rm EM}_\mu = 0$) and satisfies the constitutive relation

$$\langle j^{\rm EM}_i\rangle = \sigma\,\langle E_i\rangle\,, \tag{1.6}$$

for small departures from equilibrium. Here σ is the (DC) *electrical conductivity*,

And in theories containing one or more conserved "flavor" currents, j^α_μ, which are not coupled to dynamical gauge fields (such as baryon number or isospin currents in QCD), these currents will satisfy diffusive constitutive relations,

$$\langle j^\alpha_i\rangle = -D^{\alpha\beta}\nabla_i\langle n^\beta\rangle\,, \tag{1.7}$$

where $n^\alpha \equiv (j^\alpha)^0$ is a conserved charge density and $D \equiv \|D^{\alpha\beta}\|$ is, in general, a matrix of *diffusion constants*. Once again, the constitutive relation (1.7) holds in the local fluid rest frame; otherwise, an additional convective $\langle n^\alpha\rangle\, v_i$ term is present.

In the limit of arbitrarily small gradients (so that the scale of variation in $\langle T_{\mu\nu}\rangle$ or $\langle j_\mu\rangle$ is huge compared to microscopic length scales) and arbitrarily small departures from equilibrium, the constitutive relations (1.4), (1.6) and (1.7) may be regarded

[3]This is often termed the Landau-Lifshitz convention. In theories with additional conserved currents, such as a baryon number current, one may alternatively define the local rest frame as the frame in which there is no baryon number flux. This is the Eckart convention. As we wish to consider, among others, pure gauge theories in which no other conserved currents are present, the Landau-Lifshitz convention provides the only uniform definition of local flow.

[4]We use $(-{+}{+}{+})$ metric conventions.

JHEP11(2000)001

as definitions of the shear and bulk viscosities, electrical conductivity, and flavor diffusion constants. Alternatively, one may use linear response theory to relate non-equilibrium expectation values to equilibrium correlation functions [8]. This leads to well-known Kubo relations which express transport coefficients in terms of the zero-frequency slope of spectral densities of current-current or stress tensor-stress tensor correlation functions,

$$\eta = \frac{1}{20} \lim_{\omega\to 0} \frac{1}{\omega} \int d^4x e^{i\omega t} \langle [\pi_{lm}(t,\mathbf{x}),\, \pi_{lm}(0)] \rangle_{\rm eq}\,, \tag{1.8a}$$

$$\zeta = \frac{1}{2} \lim_{\omega\to 0} \frac{1}{\omega} \int d^4x e^{i\omega t} \langle [\mathcal{P}(t,\mathbf{x}),\, \mathcal{P}(0)] \rangle_{\rm eq}\,, \tag{1.8b}$$

$$\sigma = \frac{1}{6} \lim_{\omega\to 0} \frac{1}{\omega} \int d^4x e^{i\omega t} \langle [j_i^{\rm EM}(t,\mathbf{x}),\, j_i^{\rm EM}(0)] \rangle_{\rm eq}\,, \tag{1.8c}$$

$$D_{\alpha\beta} = \frac{1}{6} \lim_{\omega\to 0} \frac{1}{\omega} \int d^4x e^{i\omega t} \langle [j_i^{\alpha}(t,\mathbf{x}),\, j_i^{\gamma}(0)] \rangle_{\rm eq}\, \Xi^{-1}_{\gamma\beta}\,. \tag{1.8d}$$

In eq. (1.8a), $\pi_{lm} \equiv T_{lm} - \delta_{lm}\mathcal{P}$ denotes the traceless part of the stress tensor, while in eq. (1.8d), $\Xi \equiv \|\Xi_{\alpha\beta}\|$ is the "charge susceptibility" matrix describing mean-square global charge fluctuations (per unit volume),

$$\Xi_{\alpha\beta} \equiv \frac{\partial\langle n^\alpha\rangle}{\partial\mu_\beta} = \frac{\beta}{\mathcal{V}} \left[\langle N^\alpha N^\beta\rangle - \langle N^\alpha\rangle\langle N^\beta\rangle\right], \tag{1.9}$$

where $N^\alpha \equiv \int (d^3\mathbf{x}) n^\alpha$ is a conserved charge, $\mathcal{V}$ is the spatial volume, and β is the inverse temperature.

1.2 Results

1.2.1 Electrical conductivity

The high temperature electrical conductivity has the leading-log form

$$\sigma = C\, \frac{T}{e^2\, \ln e^{-1}}\,, \tag{1.10}$$

where the dimensionless coefficient C depends on the number (and relative charges) of the electrically charged matter fields which couple to the photon. The $T/(e^2\, \ln e^{-1})$ dependence of σ can be qualitatively understood as arising from the form $\sigma \sim e^2\, T^2\, \tau$, where $\tau \sim [e^4 T\, \log e^{-1}]^{-1}$ is the characteristic time scale for large-angle scattering (from either a single hard scattering or a sequence of small-angle scatterings which add up to produce a large angle deflection) or "transport mean free time".[5] This is just the classic Drude model form $\sigma \sim n\, e^2\, \tau/m$, appropriately generalized to an

[5]The transport mean free time is the inverse collision rate for large-angle scattering (i.e. an O(1) change in direction). In high temperature gauge theories, the mean free time for any scattering is dominated by very small angle scattering and is of order $(g^2T)^{-1}$, up to logarithms, while the transport mean free time is order $(g^4T \ln g^{-1})^{-1}$ [7, 9, 10, 11, 12, 17, 24, 25, 26].

species	N_{leptons}	N_{species}	$\sigma \times (e^2/T)\ln e^{-1}$
e	1	1	15.6964
e, μ	2	2	20.6566
e, μ, u, d, s	2	4	12.2870
e, μ, τ, u, d, s, c	3	19/3	12.5202
$e, \mu, \tau, u, d, s, c, b$	3	20/3	11.9719

Table 1: Leading-log conductivity for various numbers of leptonic charge carriers (N_{leptons}) and effective number of leptonic plus quark scatterers (N_{species}). The number N_{species} is a sum over all fermion fields weighted by the square of their electric charge.

ultra-relativistic setting (so $n \sim T^3$, and m is replaced by the typical energy T). Our exact results for the leading-log coefficient C, for various subsets of the fermions of the standard model, are shown in table 1. Which entry in the table to use depends on the temperature; each entry is valid when the included fermions are light ($m \ll T$) but the excluded fermions are heavy.

The dependence on matter field content is not precisely given by any simple analytic formula. But as detailed in section 4, the conductivity is approximately equal to

$$\sigma \simeq \left(\frac{12^4\, \zeta(3)^2\, \pi^{-3}\, N_{\text{leptons}}}{3\pi^2 + 32\, N_{\text{species}}} \right) \frac{T}{e^2 \ln e^{-1}}\,, \tag{1.11}$$

where N_{leptons} is the number of leptonic charge carriers (not counting anti-particles separately from particles), and N_{species} is a sum over all (Dirac) fermion fields weighted by the square of their electric charge assignments. So each leptonic species contributes 1 to N_{species}, each down type quark contributes 1/3 [which is $(-1/3)^2$ times 3 colors] and each up type quark contributes 4/3. It may be noted that this is exactly the same sum over charged species which appears in the (lowest-order) expression for the high temperature Debye screening mass for the photon,

$$m_D^2 = \frac{1}{3}\, N_{\text{species}}\, e^2 T^2\,. \tag{1.12}$$

The approximate form (1.11) is the result of a one-term variational approximation which becomes exact if the correct quantum statistics is replaced by classical Boltzmann statistics. This approximation reproduces the true leading-log coefficient to within an accuracy of better than 0.4% for all cases shown in table 1. In practice, neglect of subleading effects suppressed by powers of $1/\ln e^{-1}$ is a far larger issue than the accuracy with which eq. (1.11) reproduces the exact leading-log coefficient.

Our eq. (1.11) is similar to the expression found by Baym and Heiselberg [20]. The most significant difference is that their expression is missing the $3\pi^2$ term in the denominator. This term arises from Compton scattering and annihilation to photons — processes neglected in ref. [20].

JHEP11(2000)001

At temperatures above the QCD scale, where scattering from quarks must be included, these leading-log results neglect the contribution of quarks to the electric current density $j_\mu^{\rm EM}$ itself. This is quite a good approximation since the rate of strong interactions among quarks is much greater than their electromagnetic interactions and will wash out departures from equilibrium in quark distributions much faster than the relaxation of fluctuations in lepton distributions, which depends on electromagnetic interactions. This simplification amounts to the neglect of corrections to the coefficient C suppressed by $\alpha_{\rm EM}^2/\alpha_{\rm s}^2$. There are also relative $O(\alpha_s)$ corrections arising from QCD effects when a lepton scatters from a quark.

Weak interactions are ignored altogether in these calculations, so the results above, when applied to the standard model, are relevant at temperatures small compared to M_W, but large compared to the masses of the quarks and leptons considered. In particular, the electromagnetic mean free path for large angle scattering must be small compared to the weak interaction mean free path which, parametrically, requires that $\alpha^2 \gg \alpha_{\rm w}^2 (T/M_W)^4$.

For temperatures comparable or large compared to M_W, where the electroweak sector of the standard model is in its "unbroken" high temperature phase,[6] the dynamics of the U(1) hypercharge field may be characterized by a hypercharge conductivity in complete analogy to ordinary electromagnetism. Neglecting relative corrections suppressed by $\tan^4\theta_{\rm W}$ and $\alpha'/\alpha_{\rm s}$ and negligible effects due to Yukawa couplings of right-handed leptons, the hypercharge conductivity is determined by the hypercharge-mediated scattering of right-handed leptons. (Quarks and left-handed leptons scatter much more rapidly due to SU(2) or SU(3) interactions and hence contribute much less to the conductivity than right-handed leptons.) The appropriate generalization of eq. (1.11) has exactly the same form but with the charge e replaced by the hypercharge coupling g', $N_{\rm leptons}$ replaced by half the number of right-handed leptons, and $N_{\rm species}$ now given by the sum of the square of the hypercharge of each complex scalar field, plus half the square of the hypercharge of each chiral fermion field. For the three generations of the standard model, this means $N_{\rm leptons} = 3/2$ and $N_{\rm species} = 5 + n_{\rm s}/2$, where $n_{\rm s}$ is the number of Higgs doublets,[7] so that leading-log

[6]Depending on details of the scalar sector, there need not be any sharp electroweak phase transition. The "high temperature electroweak phase" should be understood as the regime where the effective mass of the weak gauge bosons comes predominantly from thermal fluctuations, not the Higgs condensate. In other words, $T \gtrsim v(T)$, where $v(T)$ is the (temperature dependent) Higgs expectation value.

[7]We normalize "hypercharge" Y by $Q = T_3 + Y$ (as opposed to the other convention that $Q = T_3 + Y/2$). The conductivity (1.13) does not depend on this normalization convention. In greater detail, $N_{\rm species} = 2n_{\rm s}(1/2)^2 + 3/2[(-1)^2 + 2(-1/2)^2 + 3(2/3)^2 + 3(-1/3)^2 + 6(1/6)^2]$, where the various terms in the bracket come from right-handed leptons, left-handed leptons, right-handed up type quarks, right-handed down type quarks and left-handed quarks, respectively. The Debye mass of the U(1) hypercharge gauge field again satisfies eq. (1.12), with $e^2 \to g'^2$.

JHEP11(2000)001

hypercharge conductivity is (approximately)

$$\sigma_{\rm hyper} \simeq 6^4\,\zeta(3)^2\,\pi^{-3}\left[\frac{\pi^2}{8}+\frac{20}{3}+\frac{2}{3}n_{\rm s}\right]^{-1}\left(\frac{T}{g'^2\ln g'^{-1}}\right). \tag{1.13}$$

1.2.2 Shear viscosity

The high temperature shear viscosity in a gauge theory with a simple gauge group (either abelian or non-abelian) has the leading-log form

$$\eta = \kappa\,\frac{T^3}{g^4\,\ln g^{-1}}\,, \tag{1.14}$$

where g is the gauge coupling. For the case of SU(3) gauge theory (i.e. QCD), our results for the leading-log shear viscosity coefficient κ for various numbers of fermion species are shown in table 2.

$N_{\rm f}$	$\eta\times(g^4/T^3)\ln g^{-1}$
0	27.126
1	60.808
2	86.473
3	106.664
4	122.958
5	136.380
6	147.627

Table 2: Leading-log shear viscosity as a function of the number of (fundamental representation) fermion flavors with $m \ll T$, for gauge group SU(3).

The analysis may be easily generalized to an arbitrary gauge group with $N_{\rm f}$ Dirac fermions in any given representation. Once again, the numerical results are approximately reproduced by a relatively simple analytic form which is the result of a one term variational calculation,

$$\eta \simeq 270\,d_{\rm A}\,\zeta(5)^2\left(\frac{2}{\pi}\right)^5(v^\top c^{-1}v)\,\frac{T^3}{g^4\,\ln g^{-1}}\,, \tag{1.15}$$

where c is the 2×2 matrix

$$c = (d_{\rm A}C_{\rm A}+N_{\rm f}\,d_{\rm F}C_{\rm F})\begin{bmatrix} d_{\rm A}C_{\rm A} & 0 \\ 0 & \frac{7}{4}N_{\rm f}\,d_{\rm F}C_{\rm F}\end{bmatrix} + \frac{9\pi^2}{128}\,N_{\rm f}\,d_{\rm F}\,C_{\rm F}^2\,d_{\rm A}\begin{bmatrix} 1 & -1 \\ -1 & 1\end{bmatrix}, \tag{1.16}$$

and

$$v = \begin{bmatrix} d_{\rm A} \\ \frac{15}{8}N_{\rm f}\,d_{\rm F}\end{bmatrix}. \tag{1.17}$$

Here, $d_{\rm F}$ and $C_{\rm F}$ denote the dimension and quadratic Casimir of the fermion representation, while $d_{\rm A}$ and $C_{\rm A}$ are the dimension and Casimir of the adjoint representation. (See appendix A.) In all cases studied, the expression (1.15) is accurate to within 0.7%. The two-by-two matrix structure of expression (1.15) arises from the fact that the leading-log shear viscosity is sensitive to all two-particle scattering processes: fermion-fermion, fermion-gluon, and gluon-gluon. In particular, the non-diagonal second term in eq. (1.16) arises from Compton scattering and $q\bar{q}$ annihilation to gluons, as will be described in sections 3 and 6.

JHEP11(2000)001

An earlier result of Baym, Monien, Pethick, and Ravenhall [17] coincides with eqs. (1.15)–(1.17) except that they omitted this second term in the matrix c. A later paper of Heiselberg [18] essentially agrees with our leading-log result for the shear viscosity of pure gauge theory,[8] but the later treatment of fermions in this paper also missed the Compton scattering and annihilation contributions and made additional errors not present in [17].

Plugging $C_{\rm A} = 0$ and $d_{\rm A} = d_{\rm F} = C_{\rm F} = 1$ into eq. (1.15) yields (a good approximation to) the leading-log QED result for $N_{\rm f}$ charged leptons and no quarks, which is again accurate to within 0.7%. For an e^+e^- plasma ($N_{\rm f} = 1$), this gives

$$\eta \simeq 270\,\zeta(5)^2 \left(\frac{2}{\pi}\right)^5 \left(\frac{529}{112} + \frac{128}{9\pi^2}\right) \frac{T^3}{e^4 \,\ln e^{-1}} = 187.129\,\frac{T^3}{e^4 \,\ln e^{-1}}\,. \tag{1.18}$$

The complete leading-log calculation for this case gives $\eta = 188.38\,T^3/(e^4 \,\ln e^{-1})$.

When applied to the standard model at temperatures small compared to M_W (but large compared to $\Lambda_{\rm QCD}$), the results of table 2 or eq. (1.15), with g the running QCD coupling (evaluated at a scale of order T), are relevant for hydrodynamic fluctuations in a quark-gluon plasma occurring on length scales which are large compared to the strong interaction transport mean free path of order $(g^4 T \ln g^{-1})^{-1}$, but small compared to the electromagnetic transport mean free path of order $(e^4 T \ln e^{-1})^{-1}$. In this regime, leptons may be regarded as freely streaming and decoupled from the quark-gluon plasma.

On longer length scales, large compared to the electromagnetic transport mean free path, the shear viscosity is dominated by electromagnetic scatterings of out-of-equilibrium charged leptons. [Photons do not contribute significantly because they are thermalized by $\gamma g \to q\bar{q}$ and $\gamma q \to qg$ processes, whose rates are $O(\alpha_{\rm EM}\,\alpha_{\rm s})$ and hence rapid compared to purely electromagnetic scatterings.] In this domain, the shear viscosity is approximately given by

$$\eta \simeq \left(\frac{5}{2}\right)^3 \zeta(5)^2 \left(\frac{12}{\pi}\right)^5 \left(\frac{N_{\rm leptons}}{9\pi^2 + 224 N_{\rm species}}\right) \frac{T^3}{e^4 \,\ln e^{-1}}\,. \tag{1.19}$$

This form reproduces the correct leading-log coefficient to within 0.5%, but neglects strong interaction effects which give relative corrections suppressed by α_s or $\alpha_{\rm EM}/\alpha_{\rm s}$ (as well as next-to-leading log corrections formally down by $1/\ln \alpha_{\rm EM}^{-1}$). Once again, $N_{\rm leptons}$ is the number of light leptonic species, and $N_{\rm species}$ is the sum over all light fermion fields weighted by the square of their electric charges.

The result (1.19) assumes that neutrinos may still be regarded as freely streaming and decoupled, so it is valid only on length scales small compared to the neutrino mean free path, which is of order $(M_Z/T)^4/(\alpha_W^2 T)$. On scales large compared to the

[8] The sign of the difference between the one-term ansatz result and the correct leading-log coefficient is reported incorrectly in ref. [18, appendix A]. In a related matter, ref. [18] incorrectly asserts that the exact η is a minimum of the variational problem set up in that paper; it is actually a maximum.

neutrino mean free path, the shear viscosity is dominated by neutrino transport and scales as T^4 times this mean free path,

$$\eta = O\left(\frac{M_Z^4}{\alpha_W^2 T}\right). \tag{1.20}$$

We have not calculated the precise coefficient and, to our knowledge, no quantitative calculation of neutrino viscosity is available in the literature.[9]

Finally, in the high temperature electroweak phase the viscosity, like the hypercharge conductivity, is dominated by right handed lepton transport. Neglecting relative order $\tan^4\theta_W$ and α'/α_s corrections plus negligible Yukawa coupling effects, the leading-log shear viscosity in this regime is given by eq. (1.19) with e replaced by g', $N_{\rm leptons} \to 3/2$, and $N_{\rm species} \to 5 + n_{\rm s}/2$.

1.2.3 Baryon and lepton number diffusion

To leading-log order, the fermion number diffusion constant in a QED or QCD-like gauge theory has the form

$$D_{\rm F} = A_{\rm F}\,\frac{T^{-1}}{g^4\,\ln g^{-1}}\,, \tag{1.21}$$

where g is the gauge coupling and $A_{\rm F}$ is a constant. For the case of SU(3) gauge theory, our results for the fermion number diffusion coefficient $A_{\rm F}$ for various numbers of fermion flavors are shown in table 3.

As will be discussed in detail below, the diffusion constant depends on the rate at which a fermion scatters off either another fermion or a gluon (photon) present in the high temperature plasma. In table 3, the line labeled "0" is analogous to a quenched (or valence) approximation and shows the result when only scattering off thermal gluons is included. The fairly weak dependence of the coefficient on $N_{\rm f}$ shows that in all cases the gluonic scattering contribution is dominant.

$N_{\rm f}$	$D_{\rm F} \times (g^4 T)\ln g^{-1}$
"0"	16.0597
1	14.3677
2	12.9990
3	11.8688
4	10.9197
5	10.1113
6	9.4145

Table 3: Leading-log diffusion constant for fermion number density as a function of the number of fermion flavors with $m \ll T$ in SU(3) gauge theory. The line labeled "0" shows the result when only scattering off thermal gluons is included.

As in the previous cases, these results for an SU(3) gauge theory are approximately reproduced by the simple analytic form

$$D_{\rm F} \simeq \left(\frac{2^4\,3^6\,\zeta(3)^2\,\pi^{-3}}{24 + 4N_{\rm f} + \pi^2}\right)\frac{T^{-1}}{g^4\,\ln g^{-1}}\,, \tag{1.22}$$

which is the result of a one-term variational approximation. In all cases studied this

[9] A fairly careful estimate of the neutrino mean free path has been given in ref. [27].

expression is accurate to within 0.3%. The three factors in the denominator arise, in order, from t-channel gluon exchange with a gluon, t-channel gluon exchange with a quark, and Compton scattering or annihilation to gluons.

This expression can be generalized to arbitrary simple gauge group and matter fields in any representation. The leading-log diffusion constant for the net number density of fermion flavor a is (approximately) given by

$$D_a \simeq \frac{6^5\,\zeta(3)^2}{\pi^3\,C_{\mathrm{R}_a}} \left[\sum_b^{\mathrm{f\bar{f}h}} T_{\mathrm{R}_b} \lambda_b + \frac{3\pi^2}{8}\, C_{\mathrm{R}_a} \right]^{-1} \left(\frac{T^{-1}}{g^4 \ln g^{-1}} \right), \tag{1.23}$$

where the sum is over all flavors and helicities b of the excitations that fermion a can scatter from in $ab \to ab$ processes mediated by gauge-boson exchange, including separately particles and antiparticles. (So 2 terms appear for scattering off of a gauge boson, complex scalar, or Weyl fermion and 4 terms for scattering from a Dirac fermion.) We have introduced the notation "$\mathrm{f\bar{f}h}$" over the sum as a reminder that the sum includes flavors [f], anti-flavors if distinct [$\bar{\mathrm{f}}$] and helicities [h]. The group representation normalization factor $T_{\mathrm{R}} \equiv C_{\mathrm{R}} d_{\mathrm{R}} / d_{\mathrm{A}}$ is defined in appendix A. The symbol λ_b is

$$\lambda_b = \begin{cases} 2, & \text{if } b \text{ is a boson}\,; \\ 1, & \text{if } b \text{ is a fermion}\,. \end{cases} \tag{1.24}$$

If the relevant scattering is by photon exchange, then $d_{\mathrm{A}} = d_R = 1$ and $e_a^2 \equiv g^2 C_{\mathrm{R}_a}$ is the squared electric charge of species a. The result (1.23) neglects any Yukawa interactions with scalar fields. Once again, the sum appearing in eq. (1.23) also appears in the lowest-order expression for the high temperature Debye mass, now generalized to an arbitrary simple gauge group and arbitrary matter content,

$$m_D^2 = \frac{1}{12} \left(\sum_b^{\mathrm{f\bar{f}h}} T_{\mathrm{R}_b} \lambda_b \right) g^2 T^2\,. \tag{1.25}$$

When applied to the standard model at temperatures small compared to M_W, the result (1.22) with $g^2 = g_{\mathrm{s}}^2$ gives (a good approximation to) the leading-log result for the diffusion constant which is appropriate for describing relaxation of fluctuations in baryon density or equivalently the net density of any particular quark flavor, on scales which are large compared to the strong interaction transport mean free path of order $(g_{\mathrm{s}}^4 T \ln g_{\mathrm{s}}^{-1})^{-1}$. If the departure from equilibrium of the various quark densities has vanishing electric charge density, then the resulting relaxation is purely diffusive. However, if the perturbation in quark densities has a net non-zero electric charge density, then electromagnetic interactions can only be neglected if the scale of the fluctuation is small compared to the the electromagnetic transport mean free path of order $(e^4 T \ln e^{-1})^{-1}$. On longer scales, the net charge density will relax at a rate affected by the electrical conductivity, while electrically neutral flavor asymmetries will relax diffusively. This will be discussed further momentarily.

The leading-log diffusion constant characterizing the relaxation of fluctuations in charged lepton densities which are electrically neutral [e.g. an excess of electron minus positron density, balanced by an equal excess in $\mu^+ - \mu^-$ number density] is given by the appropriate specialization of eq. (1.23) to QED, namely

$$D_L \simeq 6^5\,\zeta(3)^2\,\pi^{-3}\left[0 + 4N_{\rm species} + \frac{3\pi^2}{8}\right]^{-1}\left(\frac{T^{-1}}{e^4\ln e^{-1}}\right). \tag{1.26}$$

Once again, $N_{\rm species}$ is the sum over all relevant fermion fields weighted by the square of their electric charge. In eq. (1.26) and in the following eqs. (1.29)–(1.31), the first term in the square bracket arises from t channel scattering from a gauge boson, the middle term represents t channel scattering from something else and the third term arises from Compton scattering and annihilation to gauge bosons.

The relaxation of an arbitrary set of slowly-varying fluctuations n_a in net quark and (charged) lepton densities (with a labeling both quark and lepton species) is described by the coupled set of diffusion/relaxation equations

$$\frac{\partial n_a}{\partial t} = D_a\,\nabla^2 n_a - \frac{\sigma_a}{e_a}\sum_b e_b\,n_b\,, \tag{1.27}$$

where σ_a is the contribution to the conductivity due to charge carriers of species a (so that $e_a\,\mathbf{j}_a = \sigma_a\mathbf{E}$, where $\mathbf{j}_a$ is the species a particle number flux and the total conductivity $\sigma = \sum_a \sigma_a$). These equations encode the fact that, in addition to various diffusive processes, the charge density $\rho \equiv \sum_a e_a n_a$ satisfies the non-diffusive relaxation equation $\dot\rho = -\sigma\rho$, up to second order gradient corrections, showing that the conductivity is the relaxation rate for large-scale charge density fluctuations.[10] In fact (as noted by Einstein), the conductivity is directly related to the underlying diffusion constants of individual species through the simple relation[11]

$$\sigma = \sum_a e_a^2\,D_a\,\frac{\partial n_a}{\partial \mu_a} \tag{1.28}$$

[or $\sigma_a = e_a^2\,D_a\,(\partial n_a/\partial\mu_a)$]. This relation assumes that the the charge susceptibility matrix (1.9) is diagonal, as it is when all charge densities vanish. For (effectively)

[10] This, of course, immediately follows from combining the continuity equation for electric charge $\dot\rho + \nabla\cdot\mathbf{j} = 0$, the defining relation for conductivity $\mathbf{j} = \sigma\mathbf{E}$, and Gauss' law $\nabla\cdot\mathbf{E} = \rho$.

[11] This identity may be seen directly from the Kubo relations (1.8c) and (1.8d). Alternatively, a simple physical derivation (specializing for convenience to electromagnetism with a single species) is easily given. Start with the diffusion equation $\mathbf{j} = -eD\boldsymbol{\nabla} n = -eD(dn/d\mu)\boldsymbol{\nabla}\mu$. Then realize that in a constant electric field the effective chemical potential is $\mu = \mu_0 - e\mathbf{E}\cdot\mathbf{x}$. Hence $\mathbf{j} = e^2 D(dn/d\mu)\mathbf{E}$, or $\sigma = e^2 D(dn/d\mu)$.

massless fermions, $\partial n/\partial\mu = \frac{1}{3}T^2$ per Dirac fermion. Since $D_L \gg D_F$, leptons completely dominate over quarks in the above species sum. Inserting the result (1.26) for the lepton diffusion constant into the Einstein relation (1.28) reproduces our previous expression (1.11) for conductivity, as it must.

For temperatures large compared to M_W (i.e. in the high temperature electroweak phase), one may find corresponding results for lepton number diffusion by specializing the general result (1.23). If Yukawa interactions are neglected, then the relaxation of left and right-handed lepton number excesses are independent. The diffusion constant for left-handed net lepton number in high temperature electroweak theory is controlled by the $\mathrm{SU}(2)_L$ gauge interactions and (approximately) equals

$$D_{L_L} \simeq 6^5\,\zeta(3)^2\,\pi^{-3}\left[6+\frac{3}{4}\,(N_{\mathrm{f}}+2n_{\mathrm{s}})+\frac{27\pi^2}{128}\right]^{-1}\left(\frac{T^{-1}}{g_w^4\ln g_w^{-1}}\right), \tag{1.29}$$

with relative corrections of order $1/\ln g_{\mathrm{w}}^{-1}$, $\tan^2\theta_W = (g'/g_{\mathrm{w}})^2$ and α_{s}. Here, $N_{\mathrm{f}} = 12$ denotes the number of SU(2) chiral doublets and n_s is the number of scalar doublets. The corresponding diffusion constant for right-handed lepton number depends on hypercharge interactions,

$$D_{L_R} \simeq 6^5\,\zeta(3)^2\,\pi^{-3}\left[0+(20+2n_{\mathrm{s}})+\frac{3\pi^2}{8}\right]^{-1}\left(\frac{T^{-1}}{g'^4\ln g'^{-1}}\right), \tag{1.30}$$

with relative corrections of order $1/\ln g'^{-1}$ and α_{s}. Inclusion of Yukawa interactions will cause the diffusion of right- and left-handed lepton number excesses to become coupled. This, however, only becomes relevant on scales larger than the mean free path for scattering processes involving Higgs emission, absorption or exchange. In the minimal standard model, this scale is of order $[(m_\ell/M_W)^2(m_{\mathrm{t}}/M_W)^2\alpha_{\mathrm{w}}^2 T]^{-1}$, where m_ℓ is the (zero temperature) mass of the lepton species of interest and m_{t} is the top quark mass. In other words, this scale is larger than the $\mathrm{SU}(2)_L$ transport mean free path by a factor of roughly $(M_W/m_\ell)^2$.

The baryon diffusion constant for $T \gg M_W$ is still given by the previous result (1.22) [with $g = g_{\mathrm{s}}$], up to relative corrections of order $1/\ln g_{\mathrm{s}}^{-1}$. This may be rewritten as

$$D_B \simeq 6^5\,\zeta(3)^2\,\pi^{-3}\left[16+\frac{16}{3}\,N_g+\frac{2\pi^2}{3}\right]^{-1}\left(\frac{T^{-1}}{g_{\mathrm{s}}^4\ln g_{\mathrm{s}}^{-1}}\right), \tag{1.31}$$

where $N_g = 3$ is the number of generations.

These (approximations to leading-log) diffusion constants for baryon and left- or right-handed lepton number density characterize the relaxation in the high temperature electroweak phase of arbitrary fluctuations in any of these densities which are hypercharge neutral. For fluctuations having non-zero hypercharge density, one must also include the effect of the induced hypercharge electric field, leading to the same coupled relaxation equations as in (1.27), but with σ now the hypercharge conductivity (and the species indices a, b now labeling right-handed leptons, left-handed charged leptons and quark flavors). For the hypercharge conductivity, the dominant contribution to the Einstein relation (1.28) comes from right-handed leptons (since g' is the weakest coupling). Once again, one may easily check that inserting the result (1.30) for the right-handed lepton diffusion constant into the Einstein relation reproduces our previous expression (1.13) for the hypercharge conductivity.

We have not computed diffusion constants for conserved numbers carried by scalars.

Several determinations of leading-log diffusion constants have previously been reported [19, 21, 22, 23]. Of these, only Moore and Prokopec [22] included all relevant diagrams, and each of these previous calculations made errors in evaluating at least one diagram. We will discuss the differences between our treatment and these previous results in more detail in section 5.

1.2.4 $\mathrm{U}(N_\mathrm{f}) \times \mathrm{U}(N_\mathrm{f})$ flavor diffusion

In QCD (or any QCD-like theory) with N_f species of fermions, one may consider the entire set of $\mathrm{SU}(N_\mathrm{f})_\mathrm{V} \times \mathrm{SU}(N_\mathrm{f})_\mathrm{A} \times \mathrm{U}(1)_\mathrm{B} \times \mathrm{U}(1)_\mathrm{A}$ currents. The diagonal components of the $\mathrm{SU}(N_\mathrm{f})_\mathrm{V}$ currents are exactly conserved (neglecting weak interactions), while in our high temperature regime, the off-diagonal $\mathrm{SU}(N_\mathrm{f})_\mathrm{V}$ currents are approximately conserved if one neglects order $(\Delta m/T)^2$ effects, where Δm is some fermion mass difference. Similarly, conservation of the $\mathrm{SU}(N_\mathrm{f})_\mathrm{A}$ currents is spoiled only by $O(m^2/T^2)$ corrections. Consequently, the constitutive relations for the different currents must decouple,

$$\begin{aligned} \mathrm{U}(1)_\mathrm{B} &: \langle \mathbf{j}_\mathrm{B} \rangle = -D_\mathrm{B} \, \nabla \langle n_\mathrm{B} \rangle \, , \\ \mathrm{SU}(N_\mathrm{f})_\mathrm{V} &: \langle \mathbf{j}^\alpha_\mathrm{V} \rangle = -D_\mathrm{V} \, \nabla \langle n^\alpha_\mathrm{V} \rangle \, , \\ \mathrm{SU}(N_\mathrm{f})_\mathrm{A} &: \langle \mathbf{j}^\alpha_\mathrm{A} \rangle = -D_\mathrm{A} \, \nabla \langle n^\alpha_\mathrm{A} \rangle \, , \qquad (1.32) \\ \mathrm{U}(1)_\mathrm{A} &: \langle \mathbf{j}_\mathrm{A} \rangle = -D'_\mathrm{A} \, \nabla \langle n_\mathrm{A} \rangle \, , \qquad (1.33) \end{aligned}$$

and the full diffusion constant matrix (in this basis) is diagonal when power corrections vanishing like T^{-2}, as well as weak and electromagnetic interactions, are neglected.

The $\mathrm{U}(1)_\mathrm{B}$ baryon number current is almost exactly conserved,[12] so fluctuations in baryon number density will behave diffusively on length and time scales large compared to the appropriate mean free scattering time. Fluctuations in flavor asymmetries — that is, the diagonal components of the $\mathrm{SU}(N_\mathrm{f})_\mathrm{V}$ current densities — will behave diffusively on time scales large compared to QCD mean free scattering times

[12] Baryon number is exactly conserved in QCD, but its conservation is violated by electroweak effects, at rates that are exponentially small at $T \lesssim M_W$ [28, 29] and $O(\alpha_w^5 T \ln \alpha_w^{-1})$ at very high temperatures [30, 31, 32].

but small compared to the mean free time for flavor-changing weak interactions, which is of order $(m_W/T)^4/(\alpha_w^2 T)$, or (if the fluctuation is electrically charged) the electromagnetic transport mean free time of order $(e^4 T \ln e^{-1})^{-1}$.

Fluctuations in the $\mathrm{SU}(N_\mathrm{f})_\mathrm{A}$ and off-diagonal $\mathrm{SU}(N_\mathrm{f})_\mathrm{V}$ charge densities will behave diffusively on time scales large compared to mean free transport scattering times but small compared to the time scale of order T/m^2 or $T/(\delta m)^2$ where the respective symmetry breaking interactions become relevant.[13] Because of the axial anomaly, fluctuations in the $\mathrm{U}(1)_\mathrm{A}$ axial charge density may relax locally on a time scale of order $(\alpha_s^5 T \ln \alpha_s^{-1})^{-1}$ even in the massless theory. The physics behind this is completely analogous to treatment of baryon violating transitions in high temperature electroweak theory [30]–[34].[14] As for the other axial currents, fluctuations in U(1) axial charge density will relax diffusively on time scales large compared to the QCD transport mean free times, but small compared to both the perturbative T/m^2 and non-perturbative $(\alpha_s^5 T \ln \alpha_s^{-1})^{-1}$ scales where $\mathrm{U}(1)_\mathrm{A}$ violation becomes apparent. Axial charge fluctuations within this domain may be characterized by the basic diffusion equation (1.33), with a diffusion constant D'_A which is perturbatively computable.

As will be discussed in detail in section 5, to leading order in α_s the various flavor diffusion constants only depend on two-to-two particle scattering rates in the high temperature plasma. Consequently, the diffusion constants for currents corresponding the various (approximate) flavor symmetry groups are all identical,

$$D_\mathrm{B} = D_\mathrm{V} = D_\mathrm{A} = D'_\mathrm{A}\,, \tag{1.34}$$

up to relative corrections suppressed by one or more powers of α_s.

2. Kinetic theory and transport coefficients

To calculate any of the transport coefficients under consideration, correct to leading order in the interaction strength g but valid to all orders in $1/\ln g^{-1}$, it is sufficient to use a kinetic theory description for the relevant degrees of freedom. One introduces a particle distribution function $f(\mathbf{p},\mathbf{x},t)$ characterizing the phase space density of particles (which one should think of as coarse-grained on a scale large compared to $1/T$, but small compared to mean free paths). The distribution function $f(\mathbf{p},\mathbf{x},t)$ is really a multi-component vector with one component for each relevant particle

[13] So in the presence of non-zero fermion masses or mass differences, at sufficiently high temperature fluctuations in the $\mathrm{SU}(N_\mathrm{f})_\mathrm{V}$ and $\mathrm{SU}(N_\mathrm{f})_\mathrm{A}$ charge densities are "pseudo"-diffusive modes, analogous to pseudo-Goldstone bosons. Large scale fluctuations in these "almost-conserved" charge densities will satisfy a diffusion/relaxation equation of the form $\dot{n} = D\nabla^2 n - \gamma n$, where the local relaxation rate γ will be $O[(\delta m)^2/T]$ or $O(m^2/T)$, respectively.

[14] A useful discussion of this material may be found in ref. [35] [which, however, predates the realization that the transition rate per unit volume scales as $O(\alpha^5 T^4 \ln \alpha^{-1})$, not as $(\alpha T)^4$].

species (quark, gluon, etc.), but this will not be indicated explicitly until it becomes necessary. The distribution function satisfies a Boltzmann equation of the usual form

$$\left[\frac{\partial}{\partial t} + \mathbf{v_p} \cdot \frac{\partial}{\partial \mathbf{x}} + \mathbf{F}_{\rm ext} \cdot \frac{\partial}{\partial \mathbf{p}}\right] f(\mathbf{p}, \mathbf{x}, t) = -C[f] \,. \tag{2.1}$$

The external force $\mathbf{F}_{\rm ext}$ term will only be relevant in discussing the electrical conductivity. Since typical excitations in the plasma [those with $\mathbf{p} = \mathrm{O}(T)$] are highly relativistic, corrections to their dispersion relations are suppressed by $O(g^2)$ and may be neglected. Consequently, one may treat all excitations as moving at the speed of light, which means that the spatial velocity is a unit vector, $\mathbf{v_p} = \hat{\mathbf{p}} \equiv \mathbf{p}/|\mathbf{p}|$.[15]

For calculations to leading order in g and for the transport coefficients under consideration, it will be sufficient to include in the collision term $C[f]$ only two-body scattering processes, so that

$$\begin{aligned} C[f](\mathbf{p}) = \frac{1}{2} \int_{\mathbf{k},\mathbf{p}',\mathbf{k}'} & \left|M(p,k,p',k')\right|^2 (2\pi)^4 \, \delta^4(p+k-p'-k') \times \\ & \times \Big\{ f(\mathbf{p}) \, f(\mathbf{k}) \, [1{\pm}f(\mathbf{p}')] \, [1{\pm}f(\mathbf{k}')] \, - \\ & \quad - f(\mathbf{p}') \, f(\mathbf{k}') [1{\pm}f(\mathbf{p})] \, [1{\pm}f(\mathbf{k})] \Big\} \,. \end{aligned} \tag{2.2}$$

Here, p, k, etc. denote on-shell four-vectors (so that $p^0 = |\mathbf{p}|$, etc.), $M(p,k,p',k')$ is the two body scattering amplitude with non-relativistic normalization, related to the usual relativistic amplitude $\mathcal{M}$ by

$$|M(p,k,p',k')|^2 = \frac{|\mathcal{M}(p,k,p',k')|^2}{(2p_0)(2k_0)(2p_0')(2k_0')} \,, \tag{2.3}$$

and $\int_{\mathbf{p}}$ is shorthand for $\int d^3\mathbf{p}/(2\pi)^3$. The collision term is local in spacetime and all distribution functions are to be evaluated at the same spacetime position (whose coordinates have been suppressed). With multiple species of excitations there will, of course, be species-specific scattering amplitudes and multiple sums over species. As always, in the $1{\pm}f$ final state statistical factors, the upper sign applies to bosons and the lower to fermions. The overall factor of $1/2$ in (2.2) is a symmetry factor which compensates for the double counting of final states produced by interchanging $\mathbf{p}'$ and $\mathbf{k}'$.[16] Appropriate approximations for the scattering amplitudes will be discussed in the next section.

---

[15] This assumes, of course, that the particular physical quantities under consideration are dominantly sensitive to the behavior of typical "hard" excitations. We will see that this is true for the transport coefficients under discussion. However, certain other observables, such as the bulk viscosity, may be sufficiently sensitive to the dynamics of "soft" excitations with momenta $\mathbf{p} \ll T$ that their calculation requires an improved treatment which adequately describes both hard and soft degrees of freedom.

[16] In other discussions of Boltzmann equations (for example, that of ref. [26]), this symmetry factor is often tacitly included either in the transition rate $|M(p,k,p',k')|^2$, in the domain of the phase space integration, or in the sum over final state flavors. For our present purposes, making all such symmetry factors explicit is preferable.

JHEP11(2000)001

The stress-energy tensor, in this kinetic theory, equals

$$T^{\mu\nu}(x) = \int_{\mathbf{p}} v^\mu_{\mathbf{p}}\, p^\nu \, f(\mathbf{p},x)\,, \tag{2.4}$$

where $v^\mu_{\mathbf{p}} \equiv p^\mu/p^0$ is a convenient generalization of the three-vector velocity for an excitation with spatial momentum $\mathbf{p}$. ($v^\mu_{\mathbf{p}}$ is not the four-velocity and transforms non-covariantly, in just the manner required so that $(d^3\mathbf{p})\, v^\mu_{\mathbf{p}}$ does transform covariantly.) Other conserved currents are given by similar integrals over the phase-space distribution function, but with the implied species sum weighted by appropriate charges q of each species,[17]

$$j^\mu(x) = \int_{\mathbf{p}} v^\mu_{\mathbf{p}}\; q\, f(\mathbf{p},x)\,. \tag{2.5}$$

The factor p^ν which appears with $f(\mathbf{p},x)$ in eq. (2.4) reflects the fact that in this case it is the energy or momentum of an excitation which is the conserved charge. Given the Boltzmann equation (2.1) and scattering amplitudes in (2.2) which respect the microscopic conservation laws, one may easily check that the currents (2.4) and (2.5) are, in fact, conserved.

To extract transport coefficients, it is sufficient to linearize the Boltzmann equation (2.1) and examine the response of infinitesimal fluctuations in various symmetry channels. This will be described explicitly below.

But first we digress to discuss the validity of this kinetic theory approach. The Boltzmann equation (2.1) may be regarded as an effective theory, produced by integrating out (off-shell) quantum fluctuations, which is appropriate for describing the dynamics of excitations on scales large compared to $1/T$, which is the size of the typical de Broglie wavelength of an excitation. The use of kinetic theory for calculating transport coefficients may be justified in at least three different ways:

(1) One may begin with the full hierarchy of Schwinger-Dyson equations for (gauge-invariant) correlation functions in a weakly non-equilibrium state in the underlying quantum field theory. For weak coupling, one may systematically justify and then insert, a quasi-particle approximation for the spectral densities of the basic propagators, perform a suitable gradient expansion and Wigner transform and formally derive the above kinetic theory. (See refs. [36, 37, 38] and references therein.)

[17] eq. (2.5) is adequate for currents which are diagonal in the basis of species. More generally, the distribution function $f(\mathbf{p},x)$ should be viewed as a quantum density matrix for all internal degrees of freedom of an excitation. For example, in a theory with particles transforming in some representation R of the global symmetry group, the distribution function transforms under the $R \times \bar{R}$ representation. Off-diagonal components of the distribution function are relevant if one is interested in, for example, the off-diagonal parts of the $\mathrm{SU}(N_{\mathrm{f}}) \times \mathrm{SU}(N_{\mathrm{f}})$ currents. eq. (2.5) would then be generalized to $j^\mu_\alpha(x) = \int_{\mathbf{p}} v^\mu_{\mathbf{p}}\; \mathrm{tr}\,[t^\alpha f(\mathbf{p},x)]$, where t^α is the appropriate charge representation matrix.

(2) One may consider the diagrammatic expansion for the equilibrium correlator appearing in the Kubo relation (1.8) for some particular transport coefficient. After carefully analyzing the contribution of arbitrary diagrams in the kinematic limit of interest ($\mathbf{k} = 0$ and $\omega \to 0$), one may identify and resum, the infinite series of diagrams which contribute to the leading-order result. One obtains a linear integral equation, which will coincide exactly with the result obtained from linearizing the appropriate kinetic theory. This program has been carried out explicitly for scalar theories [4, 5] but not yet for gauge theories.

(3) One may directly argue (by examining equilibrium finite temperature correlators) that, for sufficiently weak coupling, the underlying high temperature quantum field theory has well-defined quasi-particles, that these quasi-particles are weakly interacting with a mean free time large compared to the actual duration of an individual collision and consequently that scattering amplitudes of these quasi-particles are well-defined to within a precision of order of the ratio of these scales. In other words, one justifies the existence of quasi-particles by looking at the spectral densities of the propagators of the basic fields, reads off their scattering amplitudes from looking at higher point correlators and writes down the kinetic theory which correctly describes the resulting quasi-particle interactions. For more discussion in the spirit of this approach see, for example, ref. [26].

Given the complexities of real-time, finite-temperature diagrammatic analysis in gauge theories (especially non-abelian theories), we find the last approach to be the most physically transparent and compelling. But this is clearly a matter of taste.

There is one important caveat in the claim that a kinetic theory of the form (2.1) can accurately describe excitations in a hot gauge theory. One may argue, as just sketched, that such a Boltzmann equation with massless dispersion relations reproduces (to within errors suppressed by powers of g) the dynamics of *typical* excitations in the plasma, namely hard excitations whose momenta are of order T. For such excitations, thermal corrections to the massless lowest-order dispersion relations are a negligible $O(g^2)$ effect. This is not true for soft excitations with momenta of order gT, or less. In gauge theories, one cannot characterize sufficiently long wavelength dynamics in terms of (quasi)-particle excitations with purely local collisions. Instead, one may think of long wavelength degrees of freedom as classical gauge field fluctuations and construct Boltzmann-Vlasov type effective theories which describe hard excitations propagating in a slowly varying classical background field. The well-known hard-thermal-loop (HTL) effective theory is of precisely this form [36], [39]–[42].

A simple kinetic theory of the form (2.1), without the complications of background gauge field fluctuations, can only be adequate for computing physical quantities which are not dominantly sensitive to soft excitations. This is true of most observables, including thermodynamic quantities such as energy density or entropy, just because phase space grows as $\mathbf{p}^2 d|\mathbf{p}|$ in (3+1)-dimensional theories. This is equally true for the transport coefficients under consideration. It will be easiest to demonstrate this *a-posteriori*. However, this insensitivity (at leading order) to soft excitations may not hold for the bulk viscosity, which is why its calculation requires a more refined analysis. (This is true even in a pure scalar theory [4, 5].)

Returning to the analysis of the Boltzmann equation (2.1), equilibrium solutions are given by

$$f^a_{\rm eq}(\mathbf{p}) = \left\{\exp\left[\beta(-u_\nu p^\nu - \mu_\alpha\, q^a_\alpha)\right] \mp 1\right\}^{-1}, \tag{2.6}$$

where β is the inverse temperature, u is the fluid four-velocity, and $\{\mu_\alpha\}$ are chemical potentials corresponding to a mutually commuting set of conserved charges. We have now included an explicit species index a and q^a_α is the value of the α'th conserved charge carried by species a. (Sums over repeated charge indices should be tacitly understood.)

Using only the fact that the scattering amplitudes respect the microscopic conservation laws, one may easily show that the collision term exactly vanishes for any such equilibrium distribution, $C[f_{\rm eq}] = 0$.

The distribution function corresponding to some non-equilibrium state which describes a small departure from equilibrium may be written as the sum of a local equilibrium distribution plus a departure from local equilibrium. This is conveniently written in the form

$$f^a(\mathbf{p},x) = f^a_0(\mathbf{p},x) + f^a_0(\mathbf{p},x)[1 \pm f^a_0(\mathbf{p},x)]\, f^a_1(\mathbf{p},x)\,. \tag{2.7}$$

Here $f^a_0(\mathbf{p},x)$ has the form of an equilibrium distribution function, but with temperature, flow velocity and chemical potentials which may vary in spacetime,

$$f^a_0(\mathbf{p},x) = \left. f^a_{\rm eq}(\mathbf{p})\right|_{\beta(x),u^\nu(x),\mu_\alpha(x)}\,. \tag{2.8}$$

Writing the departure from local equilibrium as $f_0(1 \pm f_0)\, f_1$, instead of just δf, simplifies the form of the resulting linearized collision operator (2.10). When inserted into the collision term of the Boltzmann equation, the local equilibrium part of the distribution gives no contribution, $C[f_0] = 0$, because the collision term is local in spacetime and so cannot distinguish local equilibrium from genuine equilibrium. Hence, the collision term, to first order in the departure from equilibrium, becomes a linear operator acting on the departure from local equilibrium,

$$C[f] = \mathcal{C} f_1 + O(f_1^2)\,, \tag{2.9}$$

where the action of the linearized collision operator $\mathcal{C}$ is given by

$$(\mathcal{C} f_1)^a(\mathbf{p}) \equiv \frac{1}{2} \sum_{bcd}^{\mathrm{f\bar{f}hc}} \int_{\mathbf{k},\mathbf{p}',\mathbf{k}'} \left| M^{ab}_{cd}(p,k,p',k') \right|^2 (2\pi)^4 \, \delta^4(p+k-p'-k') \times$$
$$\times f_0^a(\mathbf{p})\, f_0^b(\mathbf{k})\, [1 \pm f_0^c(\mathbf{p}')]\, [1 \pm f_0^d(\mathbf{k}')] \times$$
$$\times \left[f_1^a(\mathbf{p}) + f_1^b(\mathbf{k}) - f_1^c(\mathbf{p}') - f_1^d(\mathbf{k}') \right]. \qquad (2.10)$$

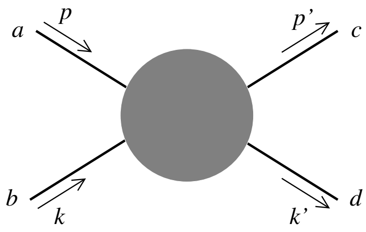

Figure 1: Momentum and species label conventions for $2 \to 2$ scattering. Time runs from left to right.

All distribution functions are evaluated at the same point in spacetime, whose coordinates have been suppressed. $M^{ab}_{cd}(p,k,p',k')$ is the scattering amplitude for species a and b, with momenta $\mathbf{p}$ and $\mathbf{k}$, respectively, to scatter into species c and d with momenta $\mathbf{p}'$ and $\mathbf{k}'$. For reference, this choice of momentum and species labels is summarized in figure 1. The "c" in the "f$\bar{\mathrm{f}}$hc" above the sum indicates that, in the application to gauge theories, the sum is over all colors of the particles represented by b, c and d, as well as flavors, anti-flavors (where distinct) and helicities.

On the left-hand side of the Boltzmann equation, the gradients acting on f_0 give a result whose size is set by either the magnitude of spacetime gradients in temperature, velocity or chemical potentials or by the magnitude of the imposed external force. So, to first order in the departure from equilibrium, the Boltzmann equation becomes an inhomogeneous linear integral equation for $f_1(\mathbf{p})$,

$$\left[\frac{\partial}{\partial t} + \hat{\mathbf{p}} \cdot \frac{\partial}{\partial \mathbf{x}} + \mathbf{F}^a_{\mathrm{ext}} \cdot \frac{\partial}{\partial \mathbf{p}} \right] f_0^a(\mathbf{p},\mathbf{x},t) = -\left(\mathcal{C} f_1\right)^a(\mathbf{p},\mathbf{x},t). \qquad (2.11)$$

In other words, f_1 is first order in gradients (or the external force). The neglected terms on the left-hand side, where derivatives act on the deviation from local equilibrium, are of second order in gradients (or external force), and do not contribute to the linearized analysis.

Each transport coefficient under consideration will depend on the departure from equilibrium f_1 resulting from a particular form of the driving terms on the left-hand side of the linearized Boltzmann equation (2.11). For conductivity, one is interested in the response to a homogeneous electric field, where $\mathbf{F}^a_{\mathrm{ext}} = q^a \mathbf{E}$. For diffusion or shear viscosity, one is interested in the response to a spatial variation in a chemical potential or the fluid flow velocity. Using the fact that

$$\mathrm{d} f_0(\mathbf{p},x) = f_0(\mathbf{p},x)[1 \pm f_0(\mathbf{p},x)]\,\mathrm{d}[\beta u_\nu p^\nu + \beta \mu_\alpha \, q^a_\alpha], \qquad (2.12)$$

one may easily see that in all three cases, the left-hand side of the linearized Boltzmann equation (2.11) has the form,[18]

$$\text{LHS} = \beta f_0^a(\mathbf{p},x)[1 \pm f_0^a(\mathbf{p},x)]q^a \, I_{i\cdots j}(\hat{\mathbf{p}}) \, X_{i\cdots j}(x) \,, \tag{2.13}$$

where the spatial tensor $X_{i\cdots j}(x)$ denotes the "driving field", namely

$$X_{i\cdots j}(x) \equiv \begin{cases} -E_i \,, & \text{(conductivity)} \\ \nabla_i \, \mu_\alpha \,, & \text{(diffusion)} \\ \frac{1}{\sqrt{6}} \left(\nabla_i u_j + \nabla_j u_i - \frac{2}{3}\delta_{ij} \nabla \cdot \mathbf{u} \right) \,, & \text{(shear viscosity)} \end{cases} \tag{2.14}$$

and $I_{i\cdots j}(\hat{\mathbf{p}})$ is the unique $\ell = 1$ or $\ell = 2$ rotationally covariant tensor depending only on the direction of $\mathbf{p}$, that is

$$I_{i\cdots j}(\hat{\mathbf{p}}) \equiv \begin{cases} \hat{p}_i \,, & \text{(conductivity/diffusion)} \\ \sqrt{\frac{3}{2}} \left(\hat{p}_i \hat{p}_j - \frac{1}{3}\delta_{ij} \right) . & \text{(shear viscosity)} \end{cases} \tag{2.15}$$

In eq. (2.13), q^a denotes the relevant charge of species a which, in the case of shear viscosity, means the magnitude of its momentum $|\mathbf{p}|$. The factor of $\sqrt{3/2}$ included in the definition (2.15) of I_{ij} [and the corresponding $1/\sqrt{6}$ factor for X_{ij} in eq. (2.14)] are inserted so that the normalization $I_{i\cdots j} I_{i\cdots j} = 1$ holds for both the $\ell = 1$ and $\ell = 2$ cases.

We will henceforth always work in the local fluid rest-frame. At any point x, the local equilibrium distribution function $f_0(\mathbf{p},x)$ then depends only on the energy $p^0 = |\mathbf{p}|$, and thus the only angular dependence on $\hat{\mathbf{p}}$ in (2.13) comes from the $\ell = 1$ or $\ell = 2$ irreducible tensor $I_{i\cdots j}(\hat{\mathbf{p}})$. Since the linearized collision operator $\mathcal{C}$ is local in spacetime and rotationally invariant (in the local fluid rest-frame at x), the departure from equilibrium must have the same angular dependence as the driving term. Consequently, given a left-hand side of the form (2.13), the function $f_1(\mathbf{p},x)$ which will solve the linearized Boltzmann equation (2.11) must have the corresponding form

$$f_1^a(\mathbf{p},x) = \beta^2 \, X_{i\cdots j}(x) \, I_{i\cdots j}(\hat{\mathbf{p}}) \chi^a(|\mathbf{p}|) \,, \tag{2.16}$$

where, for each species a, $\chi^a(|\mathbf{p}|)$ is some rotationally invariant function depending only on the energy of the excitation. The factor of β^2 is inserted for later convenience, and causes χ^a to have the same dimensions as q^a (dimensionless for conductivity

[18] For diffusion or viscosity, the time derivative term on the left-hand side may be dropped because its contribution is actually second order in spatial gradients. This follows from current (or stress-energy) conservation and the constitutive relations (1.4) or (1.7), which together imply that time derivatives of the conserved densities are related to second spatial derivatives of the conserved densities themselves.

JHEP11(2000)001

or diffusion, and dimension one for viscosity). For notational convenience we will also define

$$\chi^a_{i\cdots j}(\mathbf{p}) \equiv I_{i\cdots j}(\hat{\mathbf{p}})\chi^a(|\mathbf{p}|)\,, \tag{2.17}$$

and

$$S^a_{i\cdots j}(\mathbf{p}) \equiv -T\,q^a f^a_0(\mathbf{p},x)[1 \pm f^a_0(\mathbf{p},x)]I_{i\cdots j}(\hat{\mathbf{p}})\,, \tag{2.18}$$

so that the linearized Boltzmann equation for any particular channel under consideration can be written in the concise form

$$S^a_{i\cdots j}(\mathbf{p}) = \left(\mathcal{C}\chi_{i\cdots j}\right)^a(\mathbf{p})\,. \tag{2.19}$$

A straightforward approach for numerically solving these coupled integral equations would be to reduce them to a set of scalar equations [by contracting both sides with $I_{i\cdots j}(\hat{\mathbf{p}})$], discretize the allowed values of $|\mathbf{p}|$, compute the matrix elements $\mathcal{C}^{ab}(|\mathbf{p}|,|\mathbf{q}|)$ of the kernel of the (projected) collision operator by numerical quadrature and thereby convert (2.19) into a finite-dimensional linear matrix equation. This is a bad strategy, however, particularly for gauge theories. The problem is that the kernel $\mathcal{C}^{ab}(|\mathbf{p}|,|\mathbf{q}|)$ has (integrable) singularities and is not smooth as $|\mathbf{p}|$ crosses $|\mathbf{q}|$. Consequently it is quite difficult to avoid large discretization errors and obtain good convergence to the correct answer.

A better strategy, which is applicable to the full leading-order analysis and not just the present leading-log treatment, is to convert the linear integral equations (2.19) into an equivalent variational problem. This permits one to obtain quite accurate results using very modest basis sets. This conversion is trivial once one notes that the linear operator $\mathcal{C}$ is hermitian with respect to the natural inner product

$$(f,g) \equiv \beta^3 \sum_a^{f\bar{f}hc} \int_{\mathbf{p}} f^a(\mathbf{p})\,g^a(\mathbf{p})\,. \tag{2.20}$$

Consequently, if one defines the functional

$$Q[\chi] \equiv \Big(\chi_{i\cdots j}, S_{i\cdots j}\Big) - \frac{1}{2}\Big(\chi_{i\cdots j}, \mathcal{C}\chi_{i\cdots j}\Big)\,, \tag{2.21}$$

then the maximum value of $Q[\chi]$ occurs when $\chi^a(|\mathbf{p}|)$ satisfies the desired linear equation (2.19). For later use, note that the maximal value of the functional Q may be written in either of the forms

$$Q_{\max} = \frac{1}{2}\Big(\chi_{i\cdots j}, \mathcal{C}\chi_{i\cdots j}\Big)\bigg|_{\chi=\chi_{\max}} = \frac{1}{2}\Big(\chi_{i\cdots j}, S_{i\cdots j}\Big)\bigg|_{\chi=\chi_{\max}}\,. \tag{2.22}$$

In more explicit form, the two terms in Q are

$$\Big(\chi_{i\cdots j}, S_{i\cdots j}\Big) = -\beta^2 \sum_a^{f\bar{f}hc} \int_{\mathbf{p}} f_0(\mathbf{p})[1 \pm f_0(\mathbf{p})]q^a\chi^a(|\mathbf{p}|)\,, \tag{2.23}$$

and

$$\Big(\chi_{i\cdots j}, \mathcal{C}\chi_{i\cdots j}\Big) = \frac{\beta^3}{8}\sum_{abcd}^{f\bar{f}hc}\int_{\mathbf{p},\mathbf{k},\mathbf{p}',\mathbf{k}'} \left|M^{ab}_{cd}(p,k,p',k')\right|^2 (2\pi)^4\,\delta^4(p+k-p'-k')\,\times$$
$$\times\, f_0^a(\mathbf{p})\, f_0^b(\mathbf{k})\,[1\pm f_0^c(\mathbf{p}')]\,\left[1\pm f_0^d(\mathbf{k}')\right]\times$$
$$\times\left[\chi^a_{i\cdots j}(\mathbf{p})+\chi^b_{i\cdots j}(\mathbf{k})-\chi^c_{i\cdots j}(\mathbf{p}')-\chi^d_{i\cdots j}(\mathbf{k}')\right]^2. \qquad (2.24)$$

The sum is over all scattering processes in the plasma taking species a and b into species c and d. We have used crossing symmetry of the scattering amplitudes to write the above expression for matrix elements of $\mathcal{C}$ in a form which makes it apparent that $\mathcal{C}$ is a positive semi-definite operator. The overall factor of $1/8$ compensates for the eight times a given process appears in the multiple sum over species when all the particles are distinct (due to relabeling $a \leftrightarrow b$, $c \leftrightarrow d$ and/or $ab \leftrightarrow cd$) and supplies the appropriate symmetry factor in cases where some or all of the particles are identical. For our later discussion it will be important to note that $\mathcal{C}$ is non diagonal in the basis of species when there are $2 \leftrightarrow 2$ processes involving more than one species type.

After solving the linearized Boltzmann equation in the particular channel of interest, by maximizing $Q[\chi]$, the associated transport coefficient may be determined by inserting the resulting distribution function [given by eqs. (2.7) and (2.16)] into the stress-energy tensor (2.4) or appropriate conserved current (2.5), and comparing with the corresponding constitutive relation [eq. (1.4), (1.6) or (1.7)]. In each case, the integral over the distribution function which defines the flux (i.e. the stress tensor T_{ij} or a spatial current j_i^α) reduces to the inner product $(\chi_{i\cdots j}, S_{i\cdots j})$. Consequently, the actual value of each transport coefficient turns out to be trivially related to the maximum value (2.22) of the functional Q in the corresponding channel. Explicitly,

$$\sigma = \frac{2}{3}\,Q_{\max}\Big|_{\ell=1,\; q=q_{\rm EM}}, \qquad (2.25)$$

$$D_\alpha = \frac{2}{3}\,Q_{\max}\Big|_{\ell=1,\; q=q_\alpha}\left(\frac{\partial n_\alpha}{\partial\mu_\alpha}\right)^{-1}, \qquad (2.26)$$

$$\eta = \frac{2}{15}\,Q_{\max}\Big|_{\ell=2,\; q=|\mathbf{p}|}. \qquad (2.27)$$

The thermodynamic derivative appearing in (2.26) is the charge susceptibility,

$$\Xi_\alpha \equiv \frac{\partial n_\alpha}{\partial \mu_\alpha} = \sum_a^{f\bar{f}hc}(q^a_\alpha)^2\int_{\mathbf{p}}\beta\, f_0^a(\mathbf{p})[1\pm f_0^a(\mathbf{p})]$$
$$= \frac{1}{12}\,T^2\sum_a^{f\bar{f}hc}\lambda_a\,(q^a_\alpha)^2, \qquad (2.28)$$

where, once again, λ_a is 1 for fermions and 2 for bosons and we have specialized to the ultra-relativistic limit.

JHEP11(2000)001

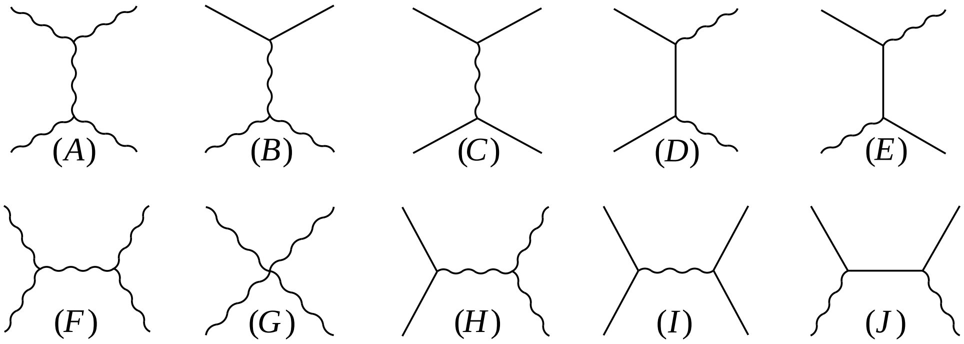

Figure 2: Leading-order diagrams for all $2 \leftrightarrow 2$ particle scattering processes in a gauge theory with fermions. Solid lines denote fermions and wiggly lines are gauge bosons. Time may be regarded as running horizontally, either way, and so a diagram such as (D) represents both $f\bar{f} \to gg$, and $gg \to f\bar{f}$. The diagrams of the first row $[(A)$–$(E)]$ contribute to the leading log transport coefficients, while the diagrams of the second row $[(F)$–$(J)]$, and all interference terms, do not.

3. Collision integrals

The full set of scattering processes which contribute at leading order in a theory with gauge and fermionic degrees of freedom are shown in figure 2. Some of these processes yield matrix elements which become singular as the momentum transfer (i.e. Mandelstam t or u) goes to zero. For instance, in a vector-like theory, the matrix element for gauge boson exchange between fermions [diagram (C)] behaves, for non-identical fermions, as

$$\mathcal{M}^2_{\text{diagram } C} \propto \frac{s^2+u^2}{t^2} \underset{\mathbf{p}\to\mathbf{p}'}{\longrightarrow} 2\,\frac{[(p+k)_\mu(p+k)^\mu]^2}{[(p-p')_\nu(p-p')^\nu]^2}\,, \tag{3.1}$$

which diverges as the inverse fourth power of the momentum transfer as $\mathbf{p}$ approaches $\mathbf{p}'$. Phase space only partially compensates, resulting in a cross section which is quadratically divergent at small $\mathbf{p}-\mathbf{p}'$. Similarly, the annihilation diagram (D) has $\mathcal{M}^2 \propto (u/t) + (t/u)$, which leads to a logarithmically IR divergent scattering cross section. However, we are not directly interested in the total scattering cross section; we need to know the size of the contribution to $\big(\chi_{i\cdots j}, \mathcal{C}\chi_{i\cdots j}\big)$ in the channels relevant to transport coefficients. As we shall review, these transport collision integrals can be less singular than the total scattering rate.

3.1 Kinematics

It is convenient to arrange the phase space integrations so that the transfer momentum is explicitly an integration variable. This will make it easy to isolate the contribution from the potentially dangerous small momentum exchange region. We choose to label the outgoing particles so that any infrared singularity in (a given term of) the square of the amplitude $|\mathcal{M}|^2$ occurs only when $(p'-p)^2 \to 0$.[19] In the collision integral (2.24) it is convenient to use the spatial δ function to perform the $\mathbf{k}'$ integration and to shift the $\mathbf{p}'$ integration into an integration over $\mathbf{p}'-\mathbf{p} \equiv \mathbf{q}$. We may write the angular integrals in spherical coordinates with $\mathbf{q}$ as the z axis and choose the x axis so $\mathbf{p}$ lies in the x-z plane. This yields

$$\begin{aligned}\Big(\chi_{i\cdots j}, \mathcal{C}\chi_{i\cdots j}\Big) = \frac{\beta^3}{(4\pi)^6} \sum_{abcd}^{\mathrm{f\bar{f}hc}} \int_0^\infty q^2 dq\, p^2 dp\, k^2 dk \int_{-1}^{1} d\cos\theta_{pq} d\cos\theta_{kq} \int_0^{2\pi} d\phi \times \\ \times \frac{1}{p\,k\,p'\,k'} \left|\mathcal{M}^{ab}_{cd}\right|^2 \delta(p+k-p'-k') \times \\ \times f_0^a(p)\, f_0^b(k) [1 \pm f_0^c(p')]\, [1 \pm f_0^d(k')] \times \\ \left[\chi^a_{i\cdots j}(\mathbf{p}) + \chi^b_{i\cdots j}(\mathbf{k}) - \chi^c_{i\cdots j}(\mathbf{p}') - \chi^d_{i\cdots j}(\mathbf{k}')\right]^2,\end{aligned} \tag{3.2}$$

where here and henceforth, p, k and q denote the magnitudes of the corresponding three-momenta (not the associated 4-momenta), $p' \equiv |\mathbf{q}+\mathbf{p}|$ and $k' \equiv |\mathbf{k}-\mathbf{q}|$ are the magnitudes of the outgoing momenta, ϕ is the azimuthal angle of $\mathbf{k}$ (and $\mathbf{k}'$) [i.e. the angle between the $\mathbf{p}$-$\mathbf{q}$ plane and the $\mathbf{k}$-$\mathbf{q}$ plane] and θ_{pq} is the plasma frame angle between $\mathbf{p}$ and $\mathbf{q}$, $\cos\theta_{pq} \equiv \hat{\mathbf{p}} \cdot \hat{\mathbf{q}}$, etc.

Following Baym et al. [17], it is convenient to introduce a dummy integration variable ω, constrained by a δ function to equal the energy transfer $p'-p$, so that

$$\delta(p+k-p'-k') = \int_{-\infty}^{\infty} d\omega\, \delta(\omega+p-p')\, \delta(\omega-k+k')\,. \tag{3.3}$$

Evaluating $p' = |\mathbf{p}+\mathbf{q}|$ in terms of p, q and $\cos\theta_{pq}$ and defining $t = \omega^2 - q^2$ (which is the usual Mandelstam variable), one finds

$$\begin{aligned}\delta(\omega+p-p') &= \frac{p'}{pq}\delta\left(\cos\theta_{pq} - \frac{\omega}{q} - \frac{t}{2pq}\right)\Theta(\omega+p)\,, \\ \delta(\omega-k+k') &= \frac{k'}{kq}\delta\left(\cos\theta_{kq} - \frac{\omega}{q} + \frac{t}{2kq}\right)\Theta(k-\omega)\,,\end{aligned} \tag{3.4}$$

where $\Theta(z)$ is the unit step function. The $\cos\theta$ integrals may now be trivially performed and yield one provided $p > \frac{1}{2}(q-\omega)$, $k > \frac{1}{2}(q+\omega)$ and $|\omega| < q$; otherwise the

[19] There is one case where this is impossible, namely, scattering between identical fermions, where the interference term between outgoing leg assignments in diagram (C) makes a contribution to the matrix element $\mathcal{M}^2 \propto s^2/ut$, which is divergent for both $t \to 0$ and $u \to 0$. As will be discussed shortly, this interference does not contribute at leading-log level. Regardless, one could also put this case in the desired form by using $s = -u - t$ and rewriting the matrix element (squared) as $(s/t) + (s/u)$, so that each piece is now singular in only one momentum region. Diagram (A) apparently has the same problem; but when one sums all $gg \to gg$ processes (only the sum is gauge invariant) one finds $\mathcal{M}^2 \propto (3 - su/t^2 - st/u^2 - tu/s^2)$, so there is no problem.

argument of a δ function has no zero for any $|\cos\theta| \leq 1$. The remaining integrals are

$$\Big(\chi_{i\cdots j}, \mathcal{C}\chi_{i\cdots j}\Big) = \frac{\beta^3}{(4\pi)^6} \sum_{abcd}^{\mathrm{f\bar{f}hc}} \int_0^\infty dq \int_{-q}^{q} d\omega \int_{\frac{q-\omega}{2}}^{\infty} dp \int_{\frac{q+\omega}{2}}^{\infty} dk \int_0^{2\pi} d\phi \times$$
$$\times \left|\mathcal{M}^{ab}_{cd}\right|^2 f_0^a(p)\, f_0^b(k)\, [1 \pm f_0^c(p')]\, [1 \pm f_0^d(k')] \times$$
$$\times \left[\chi^a_{i\cdots j}(\mathbf{p}) + \chi^b_{i\cdots j}(\mathbf{k}) - \chi^c_{i\cdots j}(\mathbf{p}') - \chi^d_{i\cdots j}(\mathbf{k}')\right]^2 , \qquad (3.5)$$

with $p' = p + \omega$ and $k' = k - \omega$. For evaluating the final factor of (3.5), note that

$$I_{i\cdots j}(\hat{\mathbf{p}})\, I_{i\cdots j}(\hat{\mathbf{k}}) = P_\ell(\cos\theta_{pk}) , \qquad (3.6)$$

where P_ℓ is the ℓ'th Legendre polynomial. We will therefore need expressions for the angles between the momenta of all species, as well as the remaining Mandelstam variables s and u, which appear in $\mathcal{M}^2$. They are

$$\begin{aligned}
\cos\theta_{pq} &= \frac{\omega}{q} + \frac{t}{2pq} , \qquad & \cos\theta_{p'q} &= \frac{\omega}{q} - \frac{t}{2p'q} , \\
\cos\theta_{kq} &= \frac{\omega}{q} - \frac{t}{2kq} , \qquad & \cos\theta_{k'q} &= \frac{\omega}{q} + \frac{t}{2k'q} , \\
\cos\theta_{pp'} &= 1 + \frac{t}{2pp'} , \qquad & \cos\theta_{kk'} &= 1 + \frac{t}{2kk'} , \\
\cos\theta_{pk} &= \cos\theta_{pq}\, \cos\theta_{kq} + \sin\theta_{pq}\, \sin\theta_{kq}\, \cos\phi , \\
\cos\theta_{pk'} &= \cos\theta_{pq}\, \cos\theta_{k'q} + \sin\theta_{pq}\, \sin\theta_{k'q} \cos\phi , \\
\cos\theta_{p'k} &= \cos\theta_{p'q} \cos\theta_{kq} + \sin\theta_{p'q} \sin\theta_{kq}\, \cos\phi , \\
\cos\theta_{p'k'} &= \cos\theta_{p'q} \cos\theta_{k'q} + \sin\theta_{p'q} \sin\theta_{k'q} \cos\phi , \qquad (3.7)
\end{aligned}$$

and

$$\begin{aligned}
s &= 2pk\,(1 - \cos\theta_{pk}) \\
&= \frac{-t}{2q^2} \left\{ (p{+}p')(k{+}k') + q^2 - \cos\phi\, \sqrt{(4pp' + t)\,(4kk' + t)} \right\} , \\
u &= -t - s . \qquad (3.8)
\end{aligned}$$

3.2 Leading-log simplifications

To compute leading-log transport coefficients, it will be sufficient to extract the small q contribution to the collision integral (3.5). For small q but generic p and k (so that $q \ll T$, $q \ll p$ and $q \ll k$), one has

$$\frac{-s}{t} \simeq \frac{u}{t} \simeq \frac{2pk}{q^2}\,(1 - \cos\phi) . \qquad (3.9)$$

The ω integral is restricted to the range $-q \leq \omega \leq q$ and will be dominated by ω/q of order one. Hence, the small q integration region in a diagram where

$\mathcal{M}^2 \propto (s^2 \text{ or } u^2)/t^2$ naively behaves like $\int dq/q^3$, a quadratic infrared divergence; while for a diagram with $\mathcal{M}^2 \propto st/t^2$ (or ut/t^2 or s^2/tu) the small q integration region naively behaves like $\int dq/q$, a logarithmic divergence. These estimates are inadequate, however, if species a and c are identical, and species b and d are also identical — that is, when both incident particles undergo small angle scattering without changing their species types. In this case, since $\mathbf{p}' - \mathbf{p} = \mathbf{q}$ is small, one has

$$\chi^a_{i\cdots j}(\mathbf{p}) - \chi^a_{i\cdots j}(\mathbf{p}') = -\mathbf{q} \cdot \nabla \chi^a_{i\cdots j}(\mathbf{p}) + O(q^2)\,, \tag{3.10}$$

and similarly for $\chi^b_{i\cdots j}(\mathbf{k}) - \chi^b_{i\cdots j}(\mathbf{k}')$. Therefore, the $[\chi^a{+}\chi^b{-}\chi^c{-}\chi^d]^2$ factor in the collision integral (3.5) will contribute a factor of q^2 to the integrand, softening the small q divergence.

This $q \to 0$ cancellation is operative for diagrams (A), (B) and (C) and converts the naive estimate of a quadratic infrared divergence into a merely logarithmic divergence. It also converts interference terms involving these diagrams, which were naively log divergent, into finite contributions. The cancellation does *not* occur for diagrams (D) and (E) which involve a change of species. For these diagrams, the naive estimate of an infrared log divergent result is correct. Interference terms involving these diagrams and the remaining diagrams (F)–(J), are infrared finite from the outset. Hence, (the squares of) all diagrams in the first row in figure 2 lead to logarithmic IR divergences in eq. (3.5), while diagrams in the second row and all interference terms, do not.

All of these logarithmic divergences become convergent when one includes the self-energies appearing on exchange lines in the diagrams. The self-energies are all of order g^2T^2. For small $q \ll T$, the g^2T^2 part of the self-energies are known as the hard thermal loop (HTL) self-energies [41, 42]. An $O(g^2T^2)$ self-energy correction on a propagator is important when the exchange momentum squared becomes of order g^2T^2, which means when $q \sim gT$. In every case, the inclusion of the self-energy reduces the size of the matrix element and serves to cut off the log divergence in the infrared. For the case of the gauge boson propagator, relevant in diagrams (A)–(C), this is discussed in [17]. The demonstration that the log is cut off for diagrams (D) and (E) has apparently not appeared in the previous literature, though the self-energy for the fermion line is well known [43]. Our analysis shows that the self-energy on the fermion line is sufficient to cut off this IR divergence as well [6]. In the current paper we will not discuss this issue in detail; nor will we treat carefully the momentum region $q \gtrsim T$, where the small q approximations which led to the conclusion that there is a log divergence break down, cutting off the log from above. Instead we will make a *leading-log* treatment, which means that we will extract the *coefficient* of the logarithmic divergence. This permits us to simultaneously take q to be small, $q \ll T$, $q \ll p$, $q \ll k$, allowing certain kinematic simplifications, while simultaneously neglecting self-energy corrections in determining the matrix elements. This approximation has been customary in almost all work in the field; in fact we

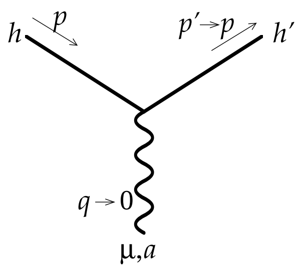

Figure 3: A generic vertex from diagrams (A)–(C) of figure 2, to be analyzed in the soft exchange limit. In this figure, the solid line denotes any sort of particle (e.g. a gauge boson or fermion) that is being scattered, and the wavy line represents the exchanged gauge boson.

are not aware of any paper which correctly goes beyond this approximation when computing a transport coefficient in a relativistic gauge theory. In a companion paper, we will treat the problem to full leading order in g [6].

3.3 Diagrams (A), (B) and (C)

Consider the gauge boson exchange diagrams (A), (B) and (C). These represent $ab \leftrightarrow ab$ processes where, in the relevant small q regime, the incoming and outgoing lines with nearly the same momenta are the same species type. The near cancellation (3.10) thus implies that the χ factors will contribute an explicit q^2 for small q. We may therefore use leading small q approximations everywhere else, together with the first *non-trivial* small q approximation for the $\chi_{i\cdots j}$ factors. As a result, the various forms which appear in the square of the matrix elements for the different diagrams (A)–(C) all become the same to leading order. In fact, in the soft exchange $(q \to 0)$ limit, the vertices in diagrams (A)-(C) take on a universal form that depends only on the color charge of the particle that is scattering, be it a gluon or quark (or scalar). Such a vertex is depicted generically in figure 3 and the associated vertex factor in the $q \to 0$ limit is[20]

$$2p^\mu g\, t^a\, \delta_{hh'}\,, \tag{3.11}$$

where t^a is the color generator in the representation of the scattering particle and h and h' are the ingoing and outgoing helicities of that particle. (The $2p$ in the factor $2p^\mu = 2pv^\mu$ is a consequence of using relativistic normalization for matrix elements.) With this $q \to 0$ Feynman rule, it is trivial to evaluate the matrix elements for the

[20] One may alternatively work directly with the full matrix elements and observe that their structure becomes identical in the $q \to 0$ limit because $(s^2+u^2)/(2t^2) \simeq -su/t^2 \simeq s^2/t^2 \simeq (4p^2k^2/q^4)\,(1-\cos\phi)^2$.

$ab \leftrightarrow ab$ scattering processes of figures (A)–(C):

$$\left|\mathcal{M}^{ab}_{ab}\right|^2_{\text{leading-log}} = A_{ab}\, \frac{s^2}{t^2}\,, \tag{3.12}$$

where the coefficient A_{ab} depends on the gauge coupling and representations of the two species,[21]

$$A_{ab} \equiv 4\, d_{\rm A}\, T_{{\rm R}_a}\, T_{{\rm R}_b} g^4\,. \tag{3.13}$$

Strictly speaking, this gives the square of the amplitude summed over incoming and outgoing gauge group indices and outgoing spins or helicities, but not summed over incoming spins or helicities, which are considered part of the species label. The corresponding contribution to the collision integral becomes

$$\begin{aligned}\Big(\chi_{i\cdots j}, \mathcal{C}\chi_{i\cdots j}\Big)^{\text{diagrams }(A-C)}_{\text{leading-log}} &= \sum_{ab}^{\rm f\bar{f}h} \frac{2A_{ab}\beta^3}{(4\pi)^6} \int_0^\infty dq \int_{-q}^{q} d\omega \int_0^\infty dk \int_0^\infty dp \int_0^{2\pi} d\phi\, \times \\ &\quad \times (1-\cos\phi)^2 \frac{4p^2k^2}{q^4}\, f_0^a(p)\,[1\pm f_0^a(p)]\, f_0^b(k)[1\pm f_0^b(k)]\, \times \\ &\quad \times \Big[\Big(\chi^a_{i\cdots j}(\mathbf{p}) - \chi^a_{i\cdots j}(\mathbf{p}')\Big) + \Big(\chi^b_{i\cdots j}(\mathbf{k}) - \chi^b_{i\cdots j}(\mathbf{k}')\Big)\Big]^2.\end{aligned} \tag{3.14}$$

As in eq. (1.23), the species sums run over all helicities and types of excitations, counting anti-particles separately from particles. The 2 next to A_{ab} arises because the sum in eq. (2.24) separately counts both $ab \to ab$ and $ab \to ba$.[22]

The leading small q approximation (3.10) to the difference of χ factors, for either $\ell = 1$ or $\ell = 2$, has the explicit form

$$\chi^a_i(\mathbf{p}) - \chi^a_i(\mathbf{p}') = -\omega\, I_i(\hat{\mathbf{p}})\, \chi^a(p)' + (\omega\, \hat{p}_i - q_i)\, \frac{\chi^a(p)}{p} + O(q^2)\,, \tag{3.15a}$$

$$\begin{aligned}\chi^a_{ij}(\mathbf{p}) - \chi^a_{ij}(\mathbf{p}') = &-\omega\, I_{ij}(\hat{\mathbf{p}})\, \chi^a(p)' + \sqrt{\frac{3}{2}}\,(2\,\omega\, \hat{p}_i\hat{p}_j - q_i\, \hat{p}_j - q_j\, \hat{p}_i)\, \frac{\chi^a(p)}{p} + \\ &+ O(q^2)\,,\end{aligned} \tag{3.15b}$$

where $\chi^a(p)'$ means $d\chi^a(p)/dp$. Expressions for $\chi^b_{i\cdots j}(\mathbf{k}) - \chi^b_{i\cdots j}(\mathbf{k}')$ are the same except for replacing $\mathbf{p}$ by $\mathbf{k}$ and changing the overall sign. For either case (and in fact, for any ℓ),

$$\Big[\chi^a_{i\cdots j}(\mathbf{p}) - \chi^a_{i\cdots j}(\mathbf{p}')\Big]^2 = \omega^2\, [\chi^a(p)']^2 + \frac{1}{2}\,\ell(\ell{+}1)\, \frac{q^2-\omega^2}{p^2}\, [\chi^a(p)]^2 + O(q^3)\,. \tag{3.16}$$

[21] If $a{=}b$, then the matrix element has a second s^2/u^2 term arising from the interchange of the outgoing lines. Swapping the $\mathbf{p}'$ and $\mathbf{k}'$ labels effectively makes the resulting matrix element twice as large.

[22] Unless $a{=}b$, in which case the extra factor of two comes from the matrix element, as noted in the previous footnote.

When expanding the last factor of eq. (3.14), there are two types of contributions to examine: those involving two χ^a or two χ^b factors, for which one may use the expression (3.16), and the cross-contributions with one χ^a and one χ^b. We will consider the cross-contributions first. As noted above, the explicit q or ω appearing in the difference (3.15) softens the small q behavior to a logarithmic divergence, so in all other factors one may work to leading order in $\mathbf{q}$. In particular one may approximate

$$\cos\theta_{pq} \simeq \cos\theta_{kq} \simeq \cos\theta_{p'q} \simeq \cos\theta_{k'q} \simeq \frac{\omega}{q}\,, \tag{3.17}$$

$$\cos\theta_{pk} \simeq \cos\theta_{p'k} \simeq \cos\theta_{pk'} \simeq \cos\theta_{p'k'} \simeq \frac{\omega^2}{q^2} + \frac{q^2-\omega^2}{q^2}\cos\phi\,. \tag{3.18}$$

Explicitly carrying out the $d\omega$ and $d\phi$ integrations, with the $(1-\cos\phi)^2$ factor from the matrix element included, one finds that all $\chi^a\chi^b$ cross terms vanish in case of $\ell = 2$ (or higher), but not for $\ell = 1$. In the $\ell = 1$ channels, however, we will only be interested in the diffusion of charge conjugation (C) odd quantum numbers (electric charge or various fermionic numbers like baryon number). In our high temperature regime, the equilibrium state may be regarded as C (or CP) invariant. Consequently, C (or CP) symmetry ensures that particles and anti-particles will have opposite departures from equilibrium, $\chi^{\overline{a}} = -\chi^a$ (where $\overline{a}$ denotes the anti-particle of species a). Hence, the sign of the cross term will be different for scatterings from fermions versus anti-fermions, so that the two contributions will cancel in the sum over species. When the scattering involves a gauge boson on one or both lines, then C symmetry ensures that the departure from equilibrium for the gauge boson is zero, so again there is no cross term. For the same reason, gauge-boson — gauge-boson scattering [diagram (A)] plays no role for conductivity or diffusion.

In either case, what remains are only the terms with two χ^a or two χ^b factors. After using (3.16) (or the same relation with $a \leftrightarrow b$ and $p \leftrightarrow k$), the ω and ϕ integrals are simple and the k integral can also be performed using

$$\int_0^\infty dk k^2 f_0^b(k)\,[1 \pm f_0^b(k)] = \lambda_b T^3\,\frac{\pi^2}{6}\,, \tag{3.19}$$

where $\lambda_b = 2$ if species b is bosonic and 1 if it is fermionic. The result is

$$\begin{aligned}
&\Big(\chi_{i\cdots j}, \mathcal{C}\chi_{i\cdots j}\Big)^{\text{diagrams }(A-C)}_{\text{leading-log}} = \\
&= \sum_{ab}^{\mathrm{f\bar{f}h}} \frac{A_{ab}}{2^9\, 3\pi^3} \int_{gT}^{T} \frac{dq}{q} \int_0^\infty dp \left[\lambda_b\, f_0^a(p)\,[1 \pm f_0^a(p)] \left(p^2\left[\chi^a(p)'\right]^2 + \ell(\ell{+}1)\,\chi^a(p)^2\right) + \right. \\
&\qquad\qquad \left. + \,(a \leftrightarrow b)\right] \qquad\qquad (3.20) \\
&= \sum_{ab}^{\mathrm{f\bar{f}h}} \frac{A_{ab}}{2^8\, 3\pi^3} \int_{gT}^{T} \frac{dq}{q} \int_0^\infty dp \lambda_b\, f_0^a(p)\,[1 \pm f_0^a(p)]\, \left(p^2\left[\chi^a(p)'\right]^2 + \ell(\ell{+}1)\,\chi^a(p)^2\right).
\end{aligned}$$

In the q integration, the upper cutoff is $q \sim T$, where the small q treatment breaks down. The lower cutoff occurs because we have not included the gauge boson's hard thermal loop self-energy in computing the matrix element. Inclusion of the self-energy makes the matrix element smaller than the vacuum amplitude and cuts off the q integration in the infrared.[23] Hence, in a leading log treatment one may simply replace the entire q integral by $\log g^{-1}$ and thereby reduce these collision integral contributions to a single one-dimensional integral.

3.4 Diagrams (D) and (E)

We begin with the annihilation diagram (D). The matrix element squared for a fermion of species f to annihilate with an anti-fermion of opposite helicity and produce two gauge bosons, $f\overline{f} \to gg$, summed over initial and final gauge group indices and gauge boson spins, is

$$\left|\mathcal{M}^{f\overline{f}}_{gg}\right|^2_{\text{leading-log}} = A_f \left(\frac{u}{t} + \frac{t}{u}\right), \tag{3.21}$$

with

$$A_f \equiv 4\, d_{\mathrm{A}}\, T_{\mathrm{R}_f}\, C_{\mathrm{R}_f} g^4 \,. \tag{3.22}$$

Interchanging labels on the outgoing legs turns (t/u) into (u/t) and so one may keep just the u/t part of the matrix element and multiply the result by two [which effectively cancels part of the overall 1/8 symmetry factor which appears in eq. (2.24)].

Since the degree of divergence is at most logarithmic, we may immediately make all available small q approximations. Namely, we may take the limits of the p and k integrations to be zero, take $f_0(p{+}\omega) \simeq f_0(p)$ and similarly $f_0(k{-}\omega) \simeq f_0(k)$, approximate $\cos\theta_{pp'} \simeq \cos\theta_{kk'} \simeq 1$ and use eqs. (3.17) and (3.18) for the various angles. The matrix element, at leading order in small q, is just

$$\frac{u}{t} \simeq \frac{2kp}{q^2}\,(1-\cos\phi)\,. \tag{3.23}$$

Making these approximations gives the following contribution to the collision integral (2.24),

$$\begin{aligned}\Big(\chi_{i\cdots j}, \mathcal{C}\chi_{i\cdots j}\Big)^{\text{diagram }(D)}_{\text{leading-log}} = \sum_f^{\text{fh}} \frac{8\, A_f\, \beta^3}{(4\pi)^6} \int_0^\infty dq \int_{-q}^{q} d\omega \int_0^\infty dk \int_0^\infty dp \int_0^{2\pi} d\phi \,\times \\ \times\,(1-\cos\phi)\frac{2pk}{q^2}\, f_0^f(p)\, f_0^{\overline{f}}(k)\,[1+f_0^g(p)][1+f_0^g(k)] \,\times \\ \times\Big\{\Big[\chi^f(p)-\chi^g(p)\Big]^2 + \Big[\chi^{\overline{f}}(k)-\chi^g(k)\Big]^2 + \\ + 2P_\ell(\cos\theta_{pk})\Big[\chi^f(p)-\chi^g(p)\Big]\Big[\chi^{\overline{f}}(k)-\chi^g(k)\Big]\Big\}\,.\end{aligned} \tag{3.24}$$

[23] This is true for both longitudinal and transverse parts of the exchanged gauge boson propagator [17].

Here χ^f is the departure from equilibrium for the fermion, $\chi^{\overline{f}}$ is for its anti-particle and χ^g is for the gauge boson. The distribution function f_0^f is the equilibrium Fermi distribution while f_0^g is the equilibrium Bose distribution. The sum runs over all fermion species and helicities, but not over anti-particles. The factor of 8 next to A_f is the 2 from the two pieces of the matrix element, times the 4 ways eq. (2.24) counts this diagram ($f\overline{f} \to gg$, $\overline{f}f \to gg$, $gg \to f\overline{f}$, $gg \to \overline{f}f$).

Using eq. (3.18) for θ_{pk}, one may easily check that

$$\int_{-q}^{q} d\omega \int_0^{2\pi} d\phi \; (1-\cos\phi)\, P_\ell(\cos\theta_{pk}) = 0 \tag{3.25}$$

for $\ell = 1$ and $\ell = 2$ (and in fact, all $\ell > 0$). Therefore the cross term involving both χ^f and $\chi^{\overline{f}}$ vanishes. For the remaining terms, the ω and ϕ integrals are trivial. For the term involving $[\chi^{\overline{f}}(k) - \chi^g(k)]^2$, one may use the symmetry of the integration region to exchange p and k. After performing the k integration with

$$\int_0^\infty dk k \, f_0^f(k)\,[1+f_0^g(k)] = \frac{\pi^2 T^2}{8}\,, \tag{3.26}$$

one finds

$$\begin{aligned}\Big(\chi_{i\cdots j}, \mathcal{C}\chi_{i\cdots j}\Big)^{\text{diagram }(D)}_{\text{leading-log}} &= \sum_f^{\text{fh}} \frac{A_f\,\beta}{2^9\,\pi^3} \int_{gT}^{T} \frac{dq}{q} \int_0^\infty dp\, p\, f_0^f(p)\,[1+f_0^g(p)] \,\times \\ &\quad \times \left\{ \Big[\chi^f(p) - \chi^g(p)\Big]^2 + \Big[\chi^{\overline{f}}(p) - \chi^g(p)\Big]^2 \right\}.\end{aligned} \tag{3.27}$$

Once again, the limits on the q integration show where the approximations we have used break down. The small q approximation breaks down for $q \gtrsim T$. Approximating the matrix element by the vacuum amplitude, without a thermal self-energy insertion on the internal fermion propagator, is invalid for $q \lesssim gT$. Below this scale the matrix element is smaller — parametrically smaller for $q \ll gT$. Our approximations are an over-estimate for $q \lesssim gT$, and the integral is cut off. For a leading log treatment, one may simply replace the q integration with $\log(T/gT) = \log g^{-1}$, which reduces the collision integral contribution (3.27) to a single integral over a quadratic form in the departures from equilibrium.

Finally, the Compton scattering diagram (E) differs only slightly from the annihilation diagram (D). The matrix element for diagram (E) is $-(s/t)$ rather than (u/t), but at leading order in small q these are equivalent. The sign of each χ associated with excitations with momentum $\mathbf{k}$ is opposite and the fermion departures from equilibrium are now either both χ^f or both $\chi^{\overline{f}}$, rather than one of each. Summing both particle and anti-particle cases, and exploiting the fact that the p–k cross-term cancels, one finds that the leading log contribution of diagram (E) is identical to that of diagram (D),

$$\Big(\chi_{i\cdots j}, \mathcal{C}\chi_{i\cdots j}\Big)^{\text{diagram }(E)}_{\text{leading-log}} = \Big(\chi_{i\cdots j}, \mathcal{C}\chi_{i\cdots j}\Big)^{\text{diagram }(D)}_{\text{leading-log}}\,. \tag{3.28}$$

Compton scattering and annihilation/pair-creation processes do not give equal contributions beyond leading log, but that does not concern us in the present paper.

4. Electrical conductivity

To find the electrical conductivity, one must determine the departure from equilibrium which is produced by an imposed electric field. For the DC conductivity, one may take the electric field $\mathbf{E}$ to be constant and neglect all spatial and temporal variation in the distribution function. As discussed in section 2, only the external force $\mathbf{F}^a_{\rm ext} = q^a\,\mathbf{E}$ contributes on the left-hand side of the linearized Boltzmann equation (2.11). Rotational invariance implies that the correction $f_1^a(\mathbf{p},x)$ to local equilibrium may be taken to have the form (2.16) which, specialized to the current case, reads

$$f_1^a(\mathbf{p},x) = -\beta^2\,(\mathbf{E}\cdot\hat{\mathbf{p}})\,\chi^a(p)\,. \tag{4.1}$$

The linearized Boltzmann equation reduces to the form $S_i^a(\mathbf{p}) = (\mathcal{C}\chi_i)^a(\mathbf{p})$, with $S_i^a(\mathbf{p}) \equiv -T q_a f_0^a(p)\,[1\pm f_0^a(p)]\,\hat{p}_i$ and $\chi_i^a(\mathbf{p}) \equiv \hat{p}_i\,\chi^a(p)$. The conductivity is given by

$$\begin{aligned}
\sigma = \frac{\mathbf{j}\cdot\mathbf{E}}{\mathbf{E}^2} &= \frac{\mathbf{E}}{\mathbf{E}^2}\cdot\sum_a^{f\bar{f}hc} q_a \int_{\mathbf{p}} \hat{\mathbf{p}}\, f_0^a(p)\,[1-f_0^a(p)]\,f_1^a(\mathbf{p}) \\
&= -\frac{1}{3}\beta^2 \sum_a^{f\bar{f}hc} q_a \int_{\mathbf{p}} f_0^a(p)\,[1-f_0^a(p)]\,\chi^a(p) \\
&= \frac{2}{3}\,Q_{\rm max}\big|_{\ell=1,q=q_{\rm EM}}\,,
\end{aligned} \tag{4.2}$$

where $Q_{\rm max}$ is the maximal value of the functional $Q[\chi] = (\chi_i, S_i) - \frac{1}{2}\,(\chi_i, \mathcal{C}\chi_i)$, first defined in eq. (2.21). [In the explicit forms shown in eq. (4.2), we have specialized to only fermionic charge carriers, as is appropriate for both pure QED and the full standard model.]

The driving term $S_i(\mathbf{p})$ in the linearized Boltzmann equation is charge conjugation (C) odd and therefore the departure from equilibrium $\chi(\mathbf{p})$ must likewise be C odd.[24] Hence, $\chi^{e^-}(p) = -\chi^{e^+}(p)$, while $\chi^\gamma(p) = 0$. In our high temperature regime, the departure from equilibrium will also be identical for different helicities of the same species and for different leptons of the same charge if there are multiple light lepton species, so that $\chi^{\mu^+} = \chi^{e^+}$, etc. If there are active quark species, then rapid QCD scattering processes (on the time scale of the relevant electromagnetic interac-

[24] Alternatively, $S_i(\mathbf{p})$ is CP even, so $\chi_i(\mathbf{p}) = \hat{p}_i\chi(p)$ is CP even, which means $\chi(p)$ itself is CP odd.

tions) ensure that $\chi^q(p)/\chi^{e^+}(p) = 0$ up to $O[(\alpha_{\rm EM}/\alpha_s)^2]$ corrections, which we will neglect. (Active quarks remain relevant, however, as targets from which the charged leptons can scatter.) Hence, for this application we may regard $\chi^{e^+}(p)$ as the only independent function which must be determined.

Let $N_{\rm leptons}$ denote the number of active lepton species (so that $4N_{\rm leptons}$ is the actual number of leptonic degrees of freedom) and let $N_{\rm species} = \frac{1}{4}\sum_a (q_a/e)^2$ denote the sum over all Dirac fermion fields weighted by the square of their electric charge assignments. Then, using the definition (2.21) of $Q[\chi]$ and the leading-log forms (3.20) and (3.27) for the relevant contributions to the collision integral, the explicit form of the functional $Q[\chi]$ becomes

$$
\begin{aligned}
\frac{Q[\chi^{e^+}]}{N_{\rm leptons}} = &-\frac{2\beta^2 e}{\pi^2}\int_0^\infty dp f_0^e(p)[1-f_0^e(p)]p^2\chi^{e^+}(p) - \\
&-(e^4\ln e^{-1})\,\frac{N_{\rm species}}{24\pi^3}\int_0^\infty dp f_0^e(p)[1-f_0^e(p)]\left\{p^2[\chi^{e^+}(p)']^2 + 2\,\chi^{e^+}(p)^2\right\} - \\
&-(e^4\ln e^{-1})\,\frac{\beta}{32\pi^3}\int_0^\infty dpp\, f_0^e(p)\,[1+f_0^\gamma(p)]\chi^{e^+}(p)^2\,.
\end{aligned}
\tag{4.3}
$$

Varying the above leading-log approximation to $Q[\chi^{e^+}]$ with respect to χ^{e^+} generates an ordinary differential equation for χ^{e^+}, as was noted in the context of shear viscosity by Heiselberg [18]. One option would be to solve that differential equation numerically. However, we find it both numerically and conceptually more convenient to instead directly attack the variational problem itself. This is also good practice for going beyond leading-log order, where the variational problem does not reduce to simple differential equations.

Since every term in this leading log form for $Q[\chi^{e^+}]$ is a one dimensional integral over p, it is possible to perform the maximization directly by discretizing values of p and then maximizing the resulting discrete quadratic form depending on a finite set of values of $\chi^{e^+}(p)$. This is completely straightforward, but requires a very fine discretization in order to determine $Q_{\rm max}$ with high accuracy. Another approach, which is both efficient and remains practical when applied to the full leading order in g calculation, is to maximize $Q[\chi^{e^+}]$ within a variational subspace given by the vector space spanned by a suitable set of basis functions, $\{\phi^{(m)}(p)\}$. In other words, one uses an ansatz

$$
\chi^{e^+}(p) = \sum_{m=1}^{N} a_m\,\phi^{(m)}(p)\,, \tag{4.4}
$$

where N is the size of the basis set considered and the coefficients a_m are variational parameters which will be tuned to maximize $Q[\chi^{e^+}]$. Inserting the ansatz (4.4) into the functional (4.3) produces an N-dimensional quadratic form,

$$\tilde{Q}[\{a_m\}] = \sum_{m=1}^{N} a_m\, \tilde{S}_m - \frac{1}{2} \sum_{m,n=1}^{N} a_m\, \tilde{C}_{mn}\, a_n\,, \tag{4.5}$$

where the basis set components of the source vector, $\tilde{S}_m \equiv (S_i, \phi_i^{(m)})$ and of the linearized collision operator, $\tilde{C}_{mn} \equiv (\phi_i^{(m)}, \mathcal{C}\phi_i^{(n)})$ may be read off from the previous expression (4.3). Maximizing $\tilde{Q}$ is now a trivial linear algebra exercise which gives $a = \tilde{C}^{-1}\,\tilde{S}$ and

$$\sigma = \frac{2}{3}\,\tilde{Q}_{max} = \frac{1}{3}\, a \cdot \tilde{S} = \frac{1}{3}\, \tilde{S}^{\top}\, \tilde{C}^{-1}\, \tilde{S}\,, \tag{4.6}$$

where $a = \|a_m\|$ and $\tilde{S} = \|\tilde{S}_m\|$ are the N-component coefficient and source vectors, respectively, in the chosen basis and $\tilde{C} \equiv \|\tilde{C}_{mn}\|$ is the (truncated) collision matrix. Given a particular choice of basis functions, the individual components $\{\tilde{S}_m\}$ and $\{\tilde{C}_{mn}\}$ may be computed by numerical quadrature and then a single $N \times N$ matrix inverse yields the conductivity via the result (4.6).

It remains to choose a good family of basis functions for the variational ansatz. There is a surprisingly good *single* function "basis set", namely $\phi^{(1)}(p) \equiv p/T$. Its use permits one to find analytic expressions for $\tilde{S}_1$ and $\tilde{C}_{11}$,

$$\begin{aligned} \tilde{S}_1^{\text{1-parameter}} &= -N_{\text{leptons}}\, \frac{9\zeta(3)}{\pi^2} (eT)\,, \\ \tilde{C}_{11}^{\text{1-parameter}} &= N_{\text{leptons}} \left(\frac{N_{\text{species}}}{24\pi} + \frac{\pi}{2^8} \right) (e^4 T \ln e^{-1})\,. \end{aligned} \tag{4.7}$$

When substituted into eq. (4.6), this yields our previously quoted approximate result eq. (1.11). This one-parameter variational ansatz is surprisingly accurate for several reasons. First, if one uses Boltzmann statistics instead of the correct Bose or Fermi distributions, [so that all appearances of $f_0(1 \pm f_0)$ are replaced by $e^{-p/T}$], then this one-parameter ansatz turns out to be exact. For large momenta, $p \gg T$, this modification produces negligible change in the integrands appearing in (4.3), but it seriously mangles the integrands at small momenta, $p \ll T$. However, the dominant contribution to the integrals in eq. (4.3) comes from $p/T \sim 4$, where the effects of quantum statistics are already rather small. Additionally, at smaller momenta the Boltzmann approximation turns out to over-estimate the contribution of diagram (C) to the scattering integral, but to under-estimate the contributions of diagrams (D) and (E). Hence there is some cancellation when the contributions are comparable. Finally, as in any variational approach, the error in the resulting conductivity scales as the square of the error in the function $\chi^{e^+}(p)$. For these reasons, a well chosen one-parameter ansatz does surprisingly well.

JHEP11(2000)001

We have investigated two larger basis sets, each of which contains $\chi = p/T$ as a special case.[25] One choice for an N-element basis set is

$$\phi^{(m)}(p) = \frac{(p/T)^m}{(1+p/T)^{N-1}}\,, \qquad m = 1, \ldots, N\,. \tag{4.8}$$

The second is

$$\phi^{(1)}(p) = \frac{p}{T}\,, \qquad \phi^{(m)}(p) = \frac{p}{T}\, e^{-p/(c_m T)}\,, \qquad m = 2, \ldots, N\,, \tag{4.9}$$

with

$$(c_2, c_3, c_4, \ldots) = \left(\log\frac{1}{2},\, \log\frac{3}{4},\, \log\frac{1}{4},\, \log\frac{7}{8},\, \log\frac{5}{8},\, \log\frac{3}{8},\, \log\frac{1}{8},\, \ldots\right). \tag{4.10}$$

For each basis set, we find that using the first four basis functions determines the (leading-log) value for σ with a relative error less than 10^{-5}, while six basis functions are good to better than one part in 10^6. The determination of $\chi^{e^+}(p)$ itself is also excellent; we compare the "exact" function $\chi^{e^+}(p)$ [obtained from a discretization with very large N] to the 1- and 6-parameter variational ansätze in figure 4. The error barely visible in the six parameter ansatz for χ^{e^+} at $p \lesssim T/10$ is quite irrelevant to the determination of the conductivity because this region of the integration domain contributes virtually nothing to the relevant integrals. One may show that the exact (leading-log) $\chi^{e^+}(p)$ function vanishes non-analytically as $p \to 0$ but this behavior has not been built into our choice of basis sets. Our numerical results for the leading-log conductivity have already been presented in table 1 of the summary. They are based on six test functions and are accurate to the last digit shown.

The best previous result in the literature for the leading-log electric conductivity in a relativistic plasma is that of Baym and Heiselberg [20]. Their analysis differs from ours in the following respects. First, they neglect diagrams (D) and (E) and the same-charge contributions (particle on particle or anti-particle on anti-particle) in diagram (C).[26] Second, they consider only the one-parameter ansatz, $\chi(p) = p/T$ and they determine its magnitude by integrating both sides of the Boltzmann equation against $\hat{\mathbf{p}}$, rather than against $\hat{\mathbf{p}}\chi(p)$. Their treatment is thus not a

[25]The basis sets (4.8) and (4.9) were actually selected in order to yield good results in our full leading-order calculations [6]. For that application, it is helpful to have a non-orthogonal basis of strictly positive functions. For a leading-log analysis, many other simple choices of basis set would be equally good.

[26]They argue that $e^-e^- \to e^-e^-$ and $e^+e^+ \to e^+e^+$ processes do not change the net current and so do not affect the conductivity. The final inference is incorrect except in the one-parameter ansatz. Though these collisions do not change the net current, they do change the distribution of velocities, which can then indirectly affect the rate at which the current is changed by other processes (although numerically the effect is quite small). Specifically within the one-parameter ansatz, however, the e^+ and e^- distributions are individually just normal thermal equilibrium distributions boosted parallel and anti-parallel to the electric field; and so for this restricted ansatz these scattering processes have no effect at all.

JHEP11(2000)001

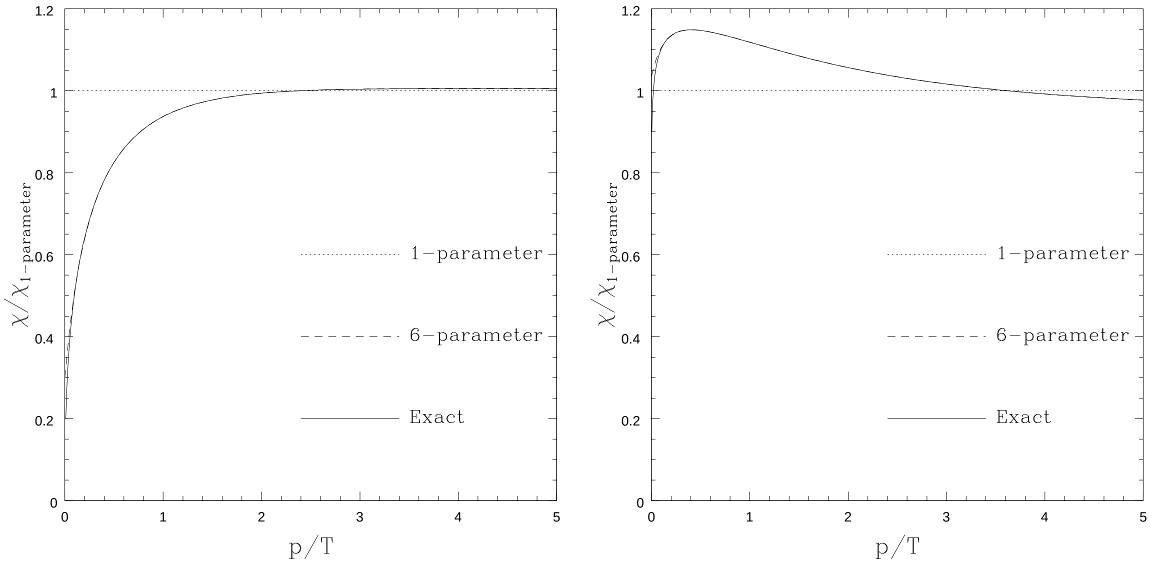

Figure 4: Comparison of the exact (leading-log) form for $\chi^e(p)$ to the one and six parameter ansatz results, for the case of an e^+e^- plasma (left) and a three lepton and five quark plasma (right). The six-parameter ansatz curve is essentially indistinguishable from the exact curve except for $p < 0.1T$. The dashed curves look exactly the same for both of our two ansätze.

variational approximation and consequently the result for the conductivity is linearly, not quadratically, sensitive to the error in the $\chi(p)$. If we drop the contribution of diagrams (D) and (E) from our analysis, our result for σ is 7.6% lower than theirs; including all diagrams, for a pure e^+e^- plasma, our result for σ is just under half of theirs.

5. Flavor diffusion

As discussed in section 2, the determination of flavor diffusion constants exactly parallels the calculation of conductivity, except for the use of differing charge assignments appropriate for the globally conserved current of interest and an overall factor of the corresponding charge susceptibility $\Xi_\alpha \equiv \partial n_\alpha / \partial \mu_\alpha$.

We will consider a theory with a simple gauge group, some set of active matter fields (fermions and/or scalars) in arbitrary representations of the gauge group, and no other significant interactions. Hence, the net number density of each matter species (or "flavor") is a conserved charge which will relax diffusively. We will only consider flavors carried exclusively by fermions. The diffusion constant for the net number density of species a is, from eq. (2.26), given by

$$D_a = \frac{2}{3}\, Q_{\max}\Big|_{\ell=1,q=q_a} \Big/ \, \Xi_a \,, \tag{5.1}$$

where the functional $Q[\chi]$ is to be maximized in the $\ell = 1$ channel with charge ± 1 assigned to all particles or antiparticles of species a, respectively and 0 to all other excitations. To be consistent, all particles and anti-particles of species a should then also be included in the number density n^a used to define the susceptibility Ξ_a [from eq. (2.28)], giving

$$\Xi_a = \frac{\partial n_a}{\partial \mu_a} = \frac{1}{3}\, d_{\mathrm{R}_a}\, T^2 \,. \tag{5.2}$$

Once again, charge conjugation (or CP) invariance implies that the particle and antiparticle departures from equilibrium are equal and opposite, $\chi^b = -\chi^{\bar{b}}$, while the gauge boson departure from equilibrium must vanish, $\chi^g = 0$.[27]

In the leading-log approximation, the gauge boson exchange contributions (3.20) to the collision operator are diagonal in particle species. [That is, there are no $\chi^a \chi^b$ cross terms in (3.20).] And when symmetry prevents the gauge bosons from having any departure from equilibrium, the leading-log annihilation/Compton scattering contributions (3.27) to the collision operator are also diagonal in particle species. Consequently, in the case at hand, where the driving term S_i in the linearized Boltzmann equation is only non zero for species a and χ^g vanishes, the only non-zero departure from equilibrium emerging from the linearized Boltzmann equation (or the maximization of $Q[\chi]$) will be for species a.

More physically, the essential point is that in the theory under consideration, in leading-log approximation, a departure from equilibrium in the net number density for species a will relax diffusively *without* inducing a net number density in any other species. Thus, for the determination of the diffusion constant D_a, the variational functional $Q[\chi]$ may be expressed solely in terms of χ^a. Using the leading-log forms (3.20) and (3.27) for the relevant contributions to the collision integral and inserting the species a particle number as the relevant charge in the source term (2.23), the explicit form of the functional $Q[\chi]$ becomes

$$\begin{aligned}\frac{Q[\chi^a]}{d_{\mathrm{R}_a}} = &-\frac{2\beta^2}{\pi^2}\int_0^\infty dp f_0^a(p)[1-f_0^a(p)]p^2\chi^a(p) - \\ &-(g^4\ln g^{-1})\frac{C_{\mathrm{R}_a}}{96\pi^3}\left[\sum_b^{\mathrm{f\bar{f}h}} T_{\mathrm{R}_b}\lambda_b\right]\int_0^\infty dp f_0^a(p)[1-f_0^a(p)]\left\{p^2[\chi^a(p)']^2+2\chi^a(p)^2\right\} - \\ &-(g^4\ln g^{-1})\frac{C_{\mathrm{R}_a}^2\beta}{32\pi^3}\int_0^\infty dp\, p f_0^a(p)[1+f_0^g(p)]\chi^a(p)^2 \,. \end{aligned} \tag{5.3}$$

Inserting a finite basis-set expansion for $\chi^a(p)$, as in eq. (4.4), extracting the resulting basis set components for the source vector $\{\tilde{S}_m\}$ and collision matrix $\{\tilde{C}_{mn}\}$, and inverting the (truncated) collision matrix to determine $\tilde{Q}_{\max}$, proceeds exactly as described in the previous section.

[27] This follows because the gauge boson distribution, which comes from the color-singlet part of its density matrix, is charge conjugation even, while the conserved charge of interest is charge conjugation odd.

Using the same one-term ansatz $\chi^a \propto p/T$ with the functional (5.3) leads to our previously quoted analytic approximation (1.23). Specialized to an SU(3) gauge theory with $N_{\rm f}$ fundamental representation quarks, this reduces to eq. (1.22). Maximizing the above $Q[\chi^a]$ using six or more terms of either basis set (4.8) or (4.9), and the specific values $C_{\rm F} = 4/3$, $T_{\rm F} = 1/2$, and $T_{\rm A} = 3$ appropriate for SU(3), leads to the numerical values shown in table 3.

Four previous determinations of the QCD diffusion coefficient merit mention. The first is by Heiselberg [19]. Within the single parameter ansatz, $\chi^a(p) \propto p/T$, his analysis coincides with ours, except that he leaves out diagrams (D) and (E). He makes an additional factor of 16/9 error in his final value for the diffusion constant, which is therefore just more than twice ours for the case $N_{\rm f} = 6$. We are unable to trace the origin of this error; equations (9)–(12) of his paper appear correct, but (13) is not. Joyce, Prokopec and Turok [21] also treat quark diffusion. In this paper they make a leading log treatment in which they only consider diagram (C), which means they only keep the $N_{\rm f} T_{\rm F}$ part of the second term in eq. (5.3). Furthermore, they neglect the energy transfer of a collision, which effectively means that they drop the $p^2[\chi^a(p)']^2$ term in the associated integral but keep the $2[\chi^a(p)]^2$ term. Under this "approximation", it is not difficult to solve exactly for the resulting form for $\chi(p)$ without any recourse to an ansatz. Their result for the diffusion constant is about 5% higher than our result would be if we only included diagram (C) [which means retaining only the middle term in the denominator of eq. (1.22)]. In fact diagram (C) is subdominant, so their result is fairly far off; for a six quark plasma their result is 2.3 times ours and for fewer quarks it is worse. They also treat lepton diffusion, making the same approximation and a corresponding sized error. Another treatment of the baryon number diffusion constant is given by Moore and Prokopec [22]. Their analysis coincides with our treatment if we make the one-parameter ansatz $\chi^a(p) \propto p/T$. They did include diagrams (B) through (E). However, they failed to include the (1/2) symmetry factor in diagram (D) and make an algebraic error in diagram (E), so their results for these diagrams are off by almost a factor of 2, and their result for the resulting diffusion constant is about 12% smaller than ours. The treatment in another paper of Joyce, Prokopec and Turok [23] is similar to the treatment of Moore and Prokopec, but only includes diagram (C) and makes some errors in its evaluation.

6. Shear viscosity

As shown in section 2, the solution of the linearized Boltzmann equation needed to determine the shear viscosity is equivalent to the maximization of the functional

$$Q[\chi] = \Big(S_{ij}, \chi_{ij}\Big) - \frac{1}{2}\Big(\chi_{ij}, \mathcal{C}\chi_{ij}\Big)\,, \tag{6.1}$$

JHEP11(2000)001

now specialized to $\ell = 2$, with $S^a_{ij}(\mathbf{p}) = -T f^a_0(p)[1 \pm f^a_0(p)]\, |\mathbf{p}|\, I_{ij}(\hat{\mathbf{p}})$, $\chi^a_{ij}(\mathbf{p}) = I_{ij}(\hat{\mathbf{p}})\, \chi^a(p)$, $I_{ij}(\hat{\mathbf{p}}) = \sqrt{\frac{3}{2}}\, (\hat{p}_i \hat{p}_j - \frac{1}{3}\delta_{ij})$, and the linearized collision operator $\mathcal{C}$ defined by eq. (2.24). The resulting viscosity is proportional to the maximal value of $Q[\chi]$,

$$\eta = \frac{2}{15} Q_{\max} \,. \tag{6.2}$$

The source term S_{ij} is invariant under all flavor symmetries as well as charge conjugation and CP. Hence, the departures from equilibrium which solve the linearized Boltzmann equation $S_{ij} = \mathcal{C}\chi_{ij}$ (or equivalently, which maximize $Q[\chi]$) will also be invariant under these symmetries. So, for example, in QCD, every quark and anti-quark species will have the same departure from equilibrium which we will denote as χ^q, and all gluons will share another common departure χ^g. But there is no reason for χ^q to equal χ^g, nor for either one to vanish. Hence, two distinct functions must be varied independently to find the maximum of $Q[\chi]$.

Using the leading-log forms (3.20) and (3.27) for the relevant contributions to the collision integral and specializing to a QCD-like theory, the two terms in $Q[\chi^g, \chi^q]$, eq. (6.1), explicitly equal

$$\Big(S_{i\cdots j}, \chi_{i\cdots j} \Big) = -\beta^2 \pi^2 \int_0^\infty dp\, p^3 \Big\{ d_{\mathrm{A}} f^g_0(p)[1+f^g_0(p)] \chi^g(p) + \\ + 2 d_{\mathrm{F}} N_{\mathrm{f}}\, f^q_0(p)[1-f^q_0(p)] \chi^q(p) \Big\} \,, \tag{6.3}$$

and

$$\frac{\Big(\chi_{i\cdots j}, \mathcal{C}\chi_{i\cdots j}\Big)}{g^4 \ln g^{-1}} = \\ = d_{\mathrm{A}} T_{\mathrm{A}} 24\pi^3 (T_{\mathrm{A}} + N_{\mathrm{f}} T_{\mathrm{F}}) \int_0^\infty dp f^g_0(p)[1+f^g_0(p)] \left\{ p^2 [\chi^g(p)']^2 + 6 \chi^g(p)^2 \right\} + \\ + \frac{N_{\mathrm{f}}\, d_{\mathrm{A}} T_{\mathrm{F}}}{12\pi^3} (T_{\mathrm{A}} + N_{\mathrm{f}} T_{\mathrm{F}}) \int_0^\infty dp f^q_0(p)\, [1-f^q_0(p)] \left\{ p^2\, [\chi^q(p)']^2 + 6\, \chi^q(p)^2 \right\} + \\ + \frac{N_{\mathrm{f}}\, d_{\mathrm{A}} T_{\mathrm{F}} C_{\mathrm{F}} \beta}{16\pi^3} \int_0^\infty dp\, p\, f^q_0(p)\, [1+f^g_0(p)] \Big[\chi^q(p) - \chi^g(p) \Big]^2 . \tag{6.4}$$

Our approach for maximizing $Q[\chi]$ is an obvious generalization of the previous treatment used for conductivity or diffusion. To carry out the maximization within a finite-dimensional variational subspace, we expand each of the undetermined functions in a finite basis set,

$$\chi^g(p) = \sum_{m=1}^{N} a_m \phi^{(m)}(p) \,, \qquad \chi^q(p) = \sum_{m=1}^{N} a_{N+m} \phi^{(m)}(p) \,, \tag{6.5}$$

with coefficients $\{a_m\}$, $m = 1, \ldots, 2N$, that are independent variational parameters. The variational functions $\phi^{(m)}(p)$ we use for shear viscosity are p times those presented in eq. (4.8) or (4.9), because the conserved charge in question is now proportional to p. Inserting eq. (6.5) into expressions (6.3) and (6.4), one may read off the basis-set components of the source vector $\tilde{S}$ and truncated scattering matrix $\tilde{C}$,

$$\Big(S_{ij}, \chi_{ij}\Big) = \sum_m a_m \, \tilde{S}_m \,, \qquad \Big(\chi_{ij}, \mathcal{C}\chi_{ij}\Big) = \sum_{m,n} a_m \, \tilde{C}_{mn} \, a_n \,. \tag{6.6}$$

As before, one has $\tilde{Q}[\{a_m\}] = a^\top \tilde{S} - \frac{1}{2} a^\top \tilde{C} \, a$. At the maximum, the vector of coefficients $a = \tilde{C}^{-1} \tilde{S}$ and

$$\eta = \frac{2}{15} \, \tilde{Q}_{\rm max} = \frac{1}{15} \, a \cdot \tilde{S} = \frac{1}{15} \, \tilde{S}^\top \tilde{C}^{-1} \tilde{S} \,. \tag{6.7}$$

The only change from the previous cases is that a set of N basis functions $\{\phi^{(m)}\}$ now generates a $2N$ dimensional linear algebra problem. Note that non-zero block off-diagonal components of $\tilde{C}_{mn}$ (those with $m \le N < n$ or $m > N \ge n$) represent a cross-coupling between the quarks and gauge bosons. These matrix elements arise only from the last term in eq. (6.4), which was generated by pair annihilation and Compton scattering processes [diagrams (D) and (E)]. If those contributions were absent, then Q would split into separate boson and fermion pieces, and the viscosity would be a sum of two independent terms, one due to fermions and the other due to the gauge bosons.

The natural one-function ansatz is now $\phi^{(1)}(p) = p^2/T$. Once again, this exactly solves the Boltzmann equation if the $f_0[1 \pm f_0]$ quantum statistics factors are replaced by classical Boltzmann statistics. With this simple ansatz, one may evaluate the integrals in (6.3) and (6.4) analytically. One finds

$$\tilde{S} = -\frac{120 \, \zeta(5) \, T^3}{\pi^2} \begin{bmatrix} d_{\rm A} \\ \frac{15}{8} \, d_{\rm F} N_{\rm f} \end{bmatrix} , \tag{6.8}$$

and

$$\tilde{C} = \frac{\pi T^3}{9 \, d_{\rm A}} \left((d_{\rm A} C_{\rm A} + N_{\rm f} \, d_{\rm F} C_{\rm F}) \begin{bmatrix} d_{\rm A} C_{\rm A} & 0 \\ 0 & \frac{7}{4} \, N_{\rm f} \, d_{\rm F} C_{\rm F} \end{bmatrix} + \frac{9\pi^2}{128} \, N_{\rm f} \, d_{\rm F} \, C_{\rm F}^2 \, d_{\rm A} \begin{bmatrix} 1 & -1 \\ -1 & 1 \end{bmatrix} \right) \times (g^4 \ln g^{-1}) \,. \tag{6.9}$$

Except for the numerical prefactors (and $g^4 \ln g^{-1}$), these are exactly expressions (1.17) and (1.16) given in section 1. When combined with the relation (6.7), these one-term ansatz results yield the approximate form (1.15) quoted earlier.

Maximizing $Q[\chi^g, \chi^q]$ for an SU(3) theory, using six or more terms of a basis set with the form of either (4.8) or (4.9), but with each basis function multiplied by one additional factor of p, leads to the numerical values shown in table 2.

It should be noted that the role played by the final term of (6.4) is *not* to relax the traceless part of the stress tensor (or momentum flux) of the plasma. At leading log order, the traceless stress is the same before and after an annihilation (or Compton scattering) process, because the outgoing momenta of the gauge bosons approximately equal the incoming momenta of the fermions. This is why the sum of these contributions vanish if $\chi^g = \chi^q$. What these processes do is to *transfer* momentum between the fermions and the bosons. Such a transfer is important, because the gauge bosons and fermions equilibrate at different rates. The gauge bosons, with their larger gauge group Casimir, equilibrate faster than the fermions. Thus, the presence of a channel which transfers a departure from equilibrium in the slowly relaxing fermions, into a departure in the more rapidly relaxing bosons, speeds the relaxation process.

This is why our result for η is somewhat lower than that found by Baym et al. [17], who missed diagrams (D) and (E), but whose treatment otherwise coincides with ours when we use the one term ansatz. For the case of three color QCD, the difference is largest at $N_{\rm f} = 2$, where it is a 3% effect. Omitting these diagrams is significantly less important for viscosity than it is for conductivity and diffusion. This is partly because scattering via gauge boson exchange becomes more efficient at higher ℓ due to the $\ell(\ell{+}1)$ factor in eq. (3.20) and partly because the processes of diagrams (D) and (E) only indirectly affect the relaxation in this case, whereas for conductivity or diffusion the annihilation and Compton scattering processes can directly relax the relevant flux.

Abelian gauge theories are a special exception. In a QED-like theory, diagrams (A) and (B) are absent (because $C_{\rm A} = 0$) and as a result diagrams (D) and (E) are essential. Without these diagrams, photon fluctuations are not damped by any logarithmically enhanced process. If one omits these processes, then the matrix $\tilde{C}$ becomes singular and the resulting leading-log viscosity diverges. This also helps explain why the QED viscosity we find in eq. (1.18) is so large.

For a more complicated theory with a product gauge group, such as QCD plus QED, or the full standard model at temperatures above M_W, it is necessary to treat the departure from equilibrium of each species with differing gauge couplings as a distinct variable; so there are many independent χ's. There are also a large number of diagrams. However, if one of the gauge couplings is much smaller than the others, so that corrections of order of the fourth power of the ratio of couplings are negligible, then one may substantially simplify the calculation. This criterion certainly holds for QCD plus QED, where $\alpha_{\rm EM}^2 \ll \alpha_{\rm s}^2$, and it is a reasonable approximation for the standard model, where $(g'/g_{\rm w})^4 < 0.1$. In this situation, all degrees of freedom which couple to the stronger gauge group, and all gauge bosons, may be regarded as remaining in equilibrium. Hence only weakly coupled fermions — leptons for QCD plus QED, right-handed leptons for the high temperature standard model — are out of equilibrium. This approximation is valid for the more strongly interacting particles because their relaxation rates are much larger. In QCD plus QED, for example, a quark's departure from equilibrium relaxes at a rate which is $O[(\alpha_{\rm s}/\alpha_{\rm EM})^2]$ faster

JHEP11(2000)001

than the corresponding rate for the electron. This approximation is also valid for the more weakly interacting gauge bosons, such as the photon, because of the mixed weak/strong scattering processes represented by diagrams (D), (E), and (J), when the fermion is a quark, one gauge line is a gluon and the other is a photon. This process occurs at a rate of order $e^2 g_{\rm s}^2 T$, which is fast compared to the $O(e^4 T)$ (up to logs) relaxation rate of leptons. Similarly, in the hot standard model, hyper-photons scatter at a rate of order $g'^2 g_{\rm s}^2 T$ which is $O(\alpha_{\rm s}/\alpha')$ larger than the large angle scattering rates for right-handed leptons. This is the approximation we have used to obtain the viscosity results discussed in section 1 for QCD plus QED and for the standard model at high temperature.

The shear viscosity in gauge theories has previously been considered by Baym, Monien, Pethick, and Ravenhall [17]. Their treatment is quite close to ours, and correctly analyzes the scattering contributions of diagrams (A)–(C) within the single function ansatz $\chi \propto p^2$. They also explore an ansatz with $\chi \propto p^\alpha$ in an effort to test the quality of the p^2 ansatz. However, they miss diagrams (D) and (E) which, as noted above, means that their values for η are slightly too large. Shear viscosity has also been considered by Heiselberg [18]. For the case of pure glue ($N_{\rm f} = 0$), Heiselberg gives a complete treatment, solving the variational problem for χ without recourse to any ansatz. We agree with his result for the $N_{\rm f} = 0$ viscosity, except for a trivial sign error in his presentation of the difference with respect to the p^2 ansatz value. However his treatment of the non-zero $N_{\rm f}$ case contains some errors not present in [17], apparently from an incorrect treatment of statistical factors in diagram (B).

Acknowledgments

This work was supported, in part, by the U.S. Department of Energy under Grant Nos. DE-FG03-96ER40956 and DE-FG02-97ER41027.

A. Group factor notation

For any representation R of a simple gauge group, let $\{t^a\}$ denote the representation matrices of the Lie algebra generators. The normalization $T_{\rm R}$ of that representation is defined by

$$\mathrm{tr}\, t^a\, t^b \equiv T_{\rm R}\, \delta^{ab}\,. \tag{A.1}$$

The quadratic Casimir $C_{\rm R}$ is defined by

$$\sum_a (t^a)^2 \equiv C_{\rm R}\, \mathbf{1}\,. \tag{A.2}$$

The two are related by

$$T_{\rm R}\, d_G = d_{\rm R}\, C_{\rm R}\,, \tag{A.3}$$

where $d_{\rm R}$ is the dimension of the representation R and $d_G{=}d_{\rm A}$ is the dimension of the gauge group. For the fundamental representation of SU(N),

$$C_{\rm F} = \frac{N^2{-}1}{2N}\,, \qquad T_{\rm F} = \frac{1}{2}\,, \qquad d_{\rm F} = N\,, \tag{A.4}$$

while for the adjoint representation,

$$C_{\rm A} = N\,, \qquad T_{\rm A} = N\,, \qquad d_{\rm A} = N^2-1\,. \tag{A.5}$$

The above notation is most natural to non-abelian theories. However, results in the text can be translated to abelian theories by taking $d_A = 1$. Then, for each species c of charged particles, take $d_R = 1$ and identify the generator t with the charge assignment (e_c/e) of that species. The group factors are then

$$C_{{\rm R}_c} = T_{{\rm R}_c} = \frac{e_c^2}{e^2}\,, \qquad C_{\rm A} = T_{\rm A} = 0\,, \qquad d_{\rm F} = 1\,. \tag{A.6}$$

References

[1] A.G. Cohen, D.B. Kaplan and A.E. Nelson, *Progress in electroweak baryogenesis*, *Ann. Rev. Nucl. Part. Sci.* **43** (1993) 27 [hep-ph/9302210].

[2] V.A. Rubakov and M.E. Shaposhnikov, *Electroweak baryon number non-conservation in the early universe and in high-energy collisions*, *Usp. Fiz. Nauk.* **166** (1996) 493 [hep-ph/9603208].

[3] See, for example, D. Teaney and E.V. Shuryak, *An unusual space-time evolution for heavy ion collisions at high energies due to the QCD phase transition*, *Phys. Rev. Lett.* **83** (1999) 4951 [nucl-th/9904006];
D.H. Rischke, S. Bernard and J.A. Maruhn, *Relativistic hydrodynamics for heavy ion collisions, 1. General aspects and expansion into vacuum*, *Nucl. Phys.* **A 595** (1995) 346 [nucl-th/9504018]; *Relativistic hydrodynamics for heavy ion collisions, 2. Compression of nuclear matter and the phase transition to the quark-gluon plasma*, *Nucl. Phys.* **A 595** (1995) 383 [nucl-th/9504021];
S. Bernard, J.A. Maruhn, W. Greiner and D.H. Rischke, *Relativistic hydrodynamics for heavy-ion collisions: freeze-out and particle spectra*, *Nucl. Phys.* **A 605** (1996) 566 [nucl-th/9602011] and references therein.

[4] S. Jeon and L.G. Yaffe, *From quantum field theory to hydrodynamics: transport coefficients and effective kinetic theory*, *Phys. Rev.* **D 53** (1996) 5799 [hep-ph/9512263].

[5] S. Jeon, *Hydrodynamic transport coefficients in relativistic scalar field theory*, *Phys. Rev.* **D 52** (1995) 3591 [hep-ph/9409250].

JHEP11(2000)001

[6] P. Arnold, G. Moore, and L.G. Yaffe, *Transport coefficients in high temperature gauge theories, 2. Beyond leading-log*, in preparation.

[7] A. Hosoya and K. Kajantie, *Transport coefficients of QCD matter*, *Nucl. Phys.* **B 250** (1985) 666.

[8] A. Hosoya, M. Sakagami and M. Takao, *Nonequilibrium thermodynamics in field theory: transport coefficients*, *Ann. Phys. (NY)* **154** (1984) 229.

[9] S. Chakrabarty, *Transport coefficients of quark-gluon plasma*, *Pramana* **25** (1985) 673.

[10] W. Czyż and W. Florkowski, *Kinetic coefficients for quark-anti-quark plasma*, *Acta Phys. Polon.* **B17** (1986) 819.

[11] D.W. von Oertzen, *Transport coefficients in quantum chromodynamics*, *Phys. Lett.* **B 280** (1992) 103.

[12] M.H. Thoma, *Viscosity coefficient of the quark-gluon plasma in the weak coupling limit*, *Phys. Lett.* **B 269** (1991) 144.

[13] S.V. Ilin, A.D. Panferov and Y.M. Sinyukov, *The viscosity coefficient in temperature gauge theories. QCD plasma*, *Phys. Lett.* **B 227** (1989) 455.

[14] J. Ahonen and K. Enqvist, *Electrical conductivity in the early universe*, *Phys. Lett.* **B 382** (1996) 40 [hep-ph/9602357].

[15] H. Davoudiasl and E. Westphal, *Diffusion and decoherence of squarks and quarks during the electroweak phase transition*, *Phys. Lett.* **B 432** (1998) 128 [hep-ph/9802335].

[16] J. Ahonen, *Transport coefficients in the early universe*, *Phys. Rev.* **D 59** (1999) 023004 [hep-ph/9801434].

[17] G. Baym, H. Monien, C.J. Pethick and D.G. Ravenhall, *Transverse interactions and transport in relativistic quark-gluon and electromagnetic plasmas*, *Phys. Rev. Lett.* **64** (1990) 1867; *Transverse interactions and transport in quark-gluon and QED plasmas*, *Nucl. Phys.* **A 525** (1991) 415C.

[18] H. Heiselberg, *Viscosities of quark-gluon plasmas*, *Phys. Rev.* **D 49** (1994) 4739 [hep-ph/9401309].

[19] H. Heiselberg, *Color, spin and flavor diffusion in quark-gluon plasmas*, *Phys. Rev. Lett.* **72** (1994) 3013 [hep-ph/9401317].

[20] G. Baym and H. Heiselberg, *The electrical conductivity in the early universe*, *Phys. Rev.* **D 56** (1997) 5254 [astro-ph/9704214].

[21] M. Joyce, T. Prokopec and N. Turok, *Nonlocal electroweak baryogenesis, 1. Thin wall regime*, *Phys. Rev.* **D 53** (1996) 2930 [hep-ph/9410281].

JHEP11(2000)001

[22] G.D. Moore and T. Prokopec, *How fast can the wall move? a study of the electroweak phase transition dynamics*, *Phys. Rev.* **D 52** (1995) 7182 [hep-ph/9506475].

[23] M. Joyce, T. Prokopec and N. Turok, *Nonlocal electroweak baryogenesis, 2. The classical regime*, *Phys. Rev.* **D 53** (1996) 2958 [hep-ph/9410282].

[24] A. Selikhov and M. Gyulassy, *Color diffusion and conductivity in a quark-gluon plasma*, *Phys. Lett.* **B 316** (1993) 373 [nucl-th/9307007].

[25] V. Lebedev and A. Smilga, *Physica* **A181** (1992) 187.

[26] P. Arnold and L.G. Yaffe, *Effective theories for real-time correlations in hot plasmas*, *Phys. Rev.* **D 57** (1998) 1178 [hep-ph/9709449].

[27] A. Heckler and C.J. Hogan, *Neutrino heat conduction and inhomogeneities in the early universe*, *Phys. Rev.* **D 47** (1993) 4256.

[28] G. 't Hooft, *Computation of the quantum effects due to a four-dimensional pseudoparticle*, *Phys. Rev.* **D 14** (1976) 3432.

[29] P. Arnold and L. McLerran, *Sphalerons, small fluctuations and baryon number violation in electroweak theory*, *Phys. Rev.* **D 36** (1987) 581.

[30] P. Arnold, D. Son and L.G. Yaffe, *The hot baryon violation rate is $O(\alpha_W^5 T^4)$*, *Phys. Rev.* **D 55** (1997) 6264 [hep-ph/9609481].

[31] D. Bodeker, *On the effective dynamics of soft non-abelian gauge fields at finite temperature*, *Phys. Lett.* **B 426** (1998) 351 [hep-ph/9801430].

[32] P. Arnold, D.T. Son and L.G. Yaffe, *Hot B violation, color conductivity and* $\log(1/\alpha)$ *effects*, *Phys. Rev.* **D 59** (1999) 105020 [hep-ph/9810216].

[33] G.D. Moore, *The sphaleron rate: Boedeker's leading log*, *Nucl. Phys.* **B 568** (2000) 367 [hep-ph/9810313].

[34] D.F. Litim and C. Manuel, *Mean field dynamics in non-abelian plasmas from classical transport theory*, *Phys. Rev. Lett.* **82** (1999) 4981 [hep-ph/9902430].

[35] L. McLerran, E. Mottola and M. Shaposhnikov, *Sphalerons and axion dynamics in high temperature QCD*, *Phys. Rev.* **D 43** (1991) 2027.

[36] J.-P. Blaizot and E. Iancu, *Kinetic theory and quantum electrodynamics at high temperature*, *Nucl. Phys.* **B 390** (1993) 589.

[37] E. Calzetta and B.L. Hu, *Nonequilibrium quantum fields: closed time path effective action, Wigner function and Boltzmann equation*, *Phys. Rev.* **D 37** (1988) 2878.

[38] E.A. Calzetta, B.L. Hu and S.A. Ramsey, *Hydrodynamic transport functions from quantum kinetic field theory*, *Phys. Rev.* **D 61** (2000) 125013 [hep-ph/9910334].

[39] U. Heinz, *Kinetic theory for nonabelian plasmas*, *Phys. Rev. Lett.* **51** (1983) 351; *Quark-gluon transport theory, 1. The classical theory*, *Ann. Phys. (NY)* **161** (1985) 48; *Quark-gluon transport theory, 2. Color response and color correlations in a quark-gluon plasma*, *Ann. Phys. (NY)* **168** (1986) 148.

[40] E. Braaten and R.D. Pisarski, *Soft amplitudes in hot gauge theories: a general analysis*, *Nucl. Phys.* **B 337** (1990) 569.

[41] J. Frenkel and J.C. Taylor, *High temperature limit of thermal QCD*, *Nucl. Phys.* **B 334** (1990) 199.

[42] J.C. Taylor and S.M. H. Wong, *The effective action of hard thermal loops in QCD*, *Nucl. Phys.* **B 346** (1990) 115.

[43] H.A. Weldon, *Effective fermion masses of order GT in high temperature gauge theories with exact chiral invariance*, *Phys. Rev.* **D 26** (1982) 2789.